ARTICLE

Received 00th January 20xx,

Accepted 00th January 20xx

DOI: 10.1039/x0xx00000x

A New Era of LMCT: Leveraging Ligand-to-Metal Charge Transfer Excited States for Photochemical Reactions

Ann Marie May [a] and Jillian L. Dempsey *[a]

Ligand-to-metal charge transfer (LMCT) excited states are capable of undergoing a wide array of photochemical reactions, yet receive minimal attention compared to other charge transfer excited states. This work provides general criteria for designing transition metal complexes that exhibit low energy LMCT excited states and routes to drive photochemistry from these excited states. General design principles regarding metal identity, oxidation state, geometry, and ligand sets are summarized. Fundamental photoreactions from these states including visible light-induced homolysis, excited state electron transfer, and other photoinduced chemical transformations are discussed and key design principles for enabling these photochemical reactions are further highlighted. Guided by these fundamentals, this review outlines critical considerations for the future design and application of coordination complexes with LMCT excited states.

Introduction

Charge transfer excited states drive most photochemical reactions. Upon irradiation with light, these highly absorptive transitions redistribute electron density across a molecule, generating a chemical potential in the excited state capable of initiating reactivity including electron transfers, proton transfers, bond homolysis, and more.[1–11] Leveraging charge transfer excited states provides a viable pathway to induce new reactivity and harness solar energy to drive chemical reactions. Charge transfer excited states are categorized into specific classes, including metal-to-ligand charge transfer (MLCT), ligand-to-metal charge transfer (LMCT), intraligand charge transfer (ILCT) and ligand-to-ligand charge transfer (LLCT).[12–16] For MLCT, ILCT, and LLCT excited states, donor orbitals populate ligand-based acceptor orbitals. However, in LMCT excited states, metal-based acceptor orbitals are populated and leave behind oxidized ligand-based orbitals, imparting unique properties to the excited state.

Transition metal complexes with LMCT excited states have historically been underexplored compared to other charge transfer excited states, namely due to their lack of photoluminescence, short excited state lifetimes, and/or propensity for degradation in the excited state. Due to these challenges, photoactive molecules with LMCT excited states were historically disregarded and photochemists turned to complexes with MLCT excited states, like tris(2,2'-bipyridine) ruthenium(II), $[Ru(bpy)_3]^{2+}$, for their attractive long-lived excited states, reversible excited state electron transfer, and (photo)chemical stability.[13,17]

Recently, a new era for LMCT excited states has begun. A handful of transition metal complexes are now known to display chemical and photochemical stability, exhibit nanosecond lifetimes, and undergo photochemical reactions.[2,16,18–23] Despite these promising results, substantial work is still required for LMCT excited states to become robust and versatile participants in photochemical reactions. Inspired by this resurgence and overall promise of LMCT excited states, this article aims to highlight transition metal complexes with LMCT excited states and understand the photochemistry accessible from these states. This article will also highlight synthetic strategies to design complexes with low energy LMCT transitions suitable for photochemical reactions. Furthermore, strategies to enhance transition metal complex stability and extend excited state lifetimes will also be discussed, highlighting state-of-the-art literature examples. Specific classes of reactions promoted by LMCT excited states, including excited state electron transfer (ES-ET) reactions, visible light-induced homolysis (VLIH), excited state proton transfer (ES-PT), and photo-induced chemical rearrangements, will be presented.

Designing Transition Metal Complexes with Low-Lying LMCT Excited States for Photochemical Reactions

LMCT transitions occur when light promotes an electron from a ligand-based molecular orbital to a metal-based molecular orbital. These excitations are facilitated by specific electronic structures, where transition metal complexes exhibit electron-deficient metal centers and have strongly donating ligand scaffolds.[2,24] Electron deficient metal centers provide vacant low energy metal-based orbitals ripe for population. In result, excitation from a ligand-based molecular orbital to an anti-bonding metal-based d orbital (t_{2g}* or e_g*) is accessible at

[a] *Department of Chemistry, University of North Carolina at Chapel Hill, Chapel Hill, North Carolina, 27599-3290, United States*

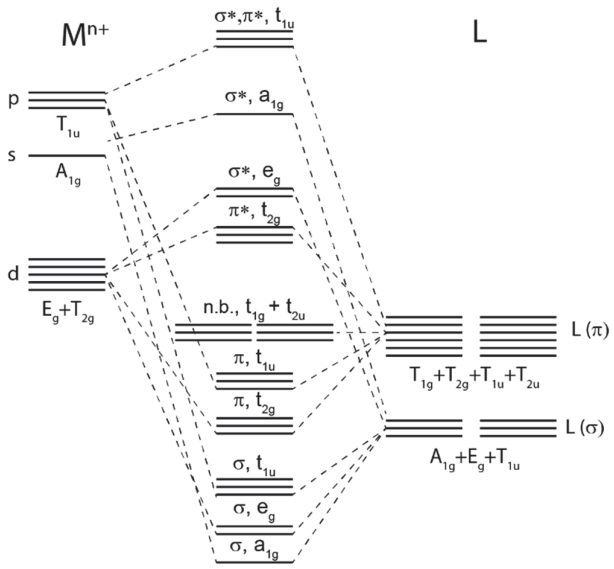

Figure 1. Molecular orbital diagram of an octahedral transition metal complex with π-donating ligands.

low energies.[2,24] Strong π donor ligands are known to promote weak to moderate ligand field splitting, where bonding orbitals are primarily ligand-based and anti-bonding orbitals are primarily metal-based (**Figure 1**, for O_h symmetry).[24] Furthermore, their anionic character supports highly oxidized metal centers. Strong σ donating ligands also give rise to coordination complexes with low-lying vacant metal-based orbitals when paired with electron deficient metal centers, albeit these metal-based orbitals exhibit non-bonding character. Therefore, to facilitate access to LMCT excited states, strongly π and σ donating ligands are commonly employed alongside electron deficient metal centers.

Classic examples of such LMCT-containing complexes include permanganate, $[MnO_4]^-$ and iridium(IV) hexabromide, $[IrBr_6]^{2-}$. For $[MnO_4]^-$, its strong π donating oxo ligands facilitate a low energy absorption within the visible region centered at 550 nm, assigned to promotion of an electron from a ligand-based t_1 non-bonding orbital to the metal-based e* orbital.[25–27] Similarly, π donating bromide ligands facilitate two sets of LMCT transitions in $[IrBr_6]^{2-}$, one in the visible (ranging from 500 to 900 nm) attributed to population of the t_{2g}* orbital and a second in the UV (spanning 250 nm to 450 nm) attributed to population of the e_g* orbital.[28–30]

While a large number of coordination complexes exhibit LMCT transitions, very few undergo excited state reactivity from their LMCT excited state, and thus only a handful have been employed as photosensitizers or photocatalysts. When identifying coordination complexes with LMCT excited states for photochemical applications, there are several considerations. The first consideration is excited state character. The nature, geometry, and (de)localization of an excited state greatly dictates its photoreactivity. For LMCT excited states, this reactivity is dictated by a shift in electron density from the ligand scaffold to the metal, producing a formally reduced metal center and oxidized ligand(s). Careful consideration of a LMCT excited states' donor and acceptor orbitals can further tune excited state properties, such as excited state reduction potentials and ligand lability.

The second consideration for enabling photosensitization and photocatalysis is excited state energetics. The relative energy of the LMCT electronic transition, with respect to other optical transitions, is important. For most photochemical reactions, photoreactivity stems from the lowest energy excited state, necessitating the construction of complexes with low-energy LMCT excited states. This criterion is rationalized by Kasha's rule which states that photoluminescence, and by extension photoreactions, occur from the lowest energy excited state of a given multiplicity – a result of fast internal conversion to the lowest energy excited state upon photoexcitation.[31,32] While there are exceptions to this rule (some of which will be discussed herein), Kasha's rule is generally applicable to most photochemical reactions and highlights a common design criterion considered when designing photoactive molecules. To meet this criterion, many complexes that exhibit low energy LMCT excited states contain strong π donating ligands. The anionic nature of π donating ligands supports high valent metal centers, enabling low-lying, metal-based antibonding orbitals that can be filled upon photoexcitation. Simultaneously, strong π donors raise the energy of the t_{2g} orbitals, resulting in small octahedral field (ΔO_h) splittings, where both metal-based orbitals are anti-bonding. In result, this pairing provides ligand-based HOMOs and metal-based LUMOs (or SOMOs) poised for low energy LMCT transitions.

However, incorporating strong π donors and high valent metal centers does not always ensure low energy LMCT excited states. The weak field splittings of these complexes promote small ΔO_h splitting, and can favor low energy d–d transitions for complexes with one or more d electrons. In addition, small ΔO_h splitting may also enable high spin configurations for some complexes, similarly enabling low energy d–d transitions. To combat these low-lying d–d transitions, strong σ donors can be incorporated to stabilize the t_{2g} orbitals and promote low spin electronic configurations. This stabilization results in larger ΔO_h splitting relative to π donors and the ligand field (metal centered, d–d) excited states that commonly deactivate LMCT excited states increase in energy relative to the charge transfer transition.[2,15] In addition to carefully tuning ligand identity and electronics, metal identity and oxidation state can similarly manipulate ΔO_h splittings, where ΔO_h splittings increase with increasing oxidation state number and principal quantum number, and change the energetics of metal-based acceptor orbitals in LMCT transitions. In result, careful consideration of ligand and metal identities can enable the design of transition metal complexes with low energy LMCT excited states.

The third consideration for constructing effective photosensitizers and photocatalysts is excited state lifetime. For some reactions, ultrafast lifetimes are sufficient to enable photochemistry, particularly when the photoreaction is unimolecular in nature. However, lifetimes on the nanosecond timescale are typically required for bimolecular reactions with substrates in the millimolar concentration range, where excited states must persist on the timescale of diffusion. A variety of

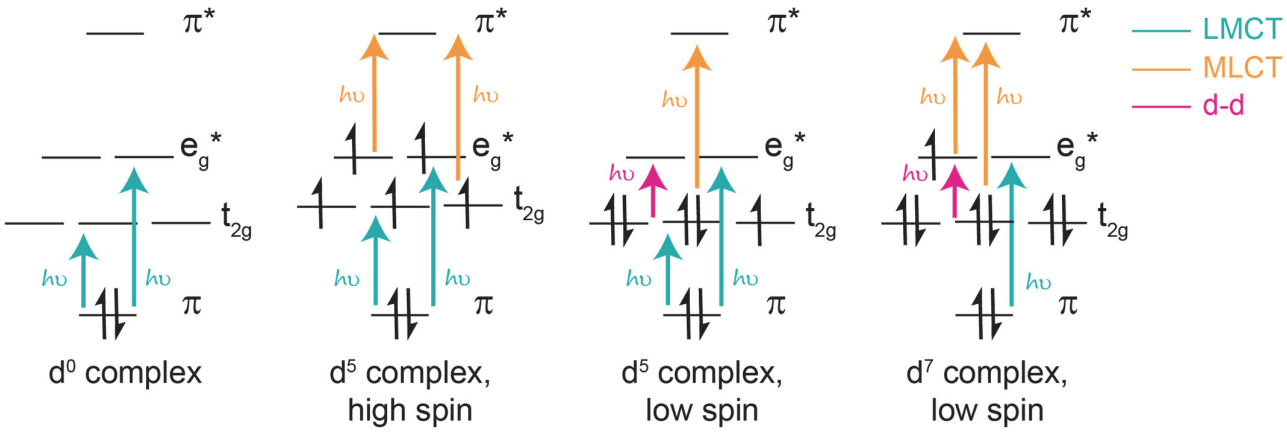

Figure 2. Examples of accessible excited states from d^0, d^5, and d^7 complexes, which most commonly exhibit LMCT. In addition, it is important to note the bonding character of the metal-based t_{2g} orbitals depends on the nature of the coordinating ligands. Strong π donors facilitate anti-bonding t_{2g} orbitals, σ donors promote non-bonding t_{2g} orbitals, and π acceptors facilitate bonding t_{2g} orbitals.

factors play into the lifetimes of these excited states, including excited state spin multiplicity and accessible nonradiative decay pathways. Metal complexes capable of intersystem crossing (e.g., from singlet to triplet excited states) are generally more likely to exhibit long-lived excited state lifetimes than complexes that cannot. Furthermore, complexes comprised of second and third row transition metals have larger ligand field splitting that first row metals. Large ligand field splittings can prevent deactivation of a charge transfer excited state through metal-centered excited states. Similarly, ligand choice also impacts ligand field splittings, as illustrated in Tanube-Sugano diagrams for specific electronic configurations.

The fourth design criterion for constructing photosensitizers and photocatalysts is (photo)stability. Most electronic transitions result in the population of anti-bonding orbitals upon photoexcitation. Therefore, in the case of many LMCT transitions, the metal-ligand bond lengths elongate and can result in ligand dissociation. For example, despite the short excited state lifetime of $[MnO_4]^-$, this molecule is capable of undergoing photoreactivity to unimolecularly produce O_2 and $[MnO_2]^-$ upon irradiation. This ultrafast photodecomposition rationalizes why it is not commonly employed as a photocatalyst or photosensitizer in photochemical reactions, as this irreversible reaction will inherently compete with more complex photoreactions of interest. Conversely, while LMCT excitation of d^5 octahedral $[IrBr_6]^{2-}$ complex populates an antibonding t_{2g} orbital, it does not showcase photochemical instability. Instead, $[IrBr_6]^{2-}$ is unstable in the ground state, where it is known to undergo substitution with water molecules and is only stable in the presence of excess bromide ions.[28] Given the challenges that arise from populating metal–ligand antibonding orbitals and transiently oxidizing ligands, it is important to employ ligands that are strongly coordinating and stable to oxidation to access transition metal complexes capable of photochemistry from low-lying LMCT excited states.

While the four criteria outlined above—excited state character, excited state energy, excited state lifetime, and photochemical stability—appear as straightforward design principles, designing transition metal complexes that possess low energy LMCT excited states capable of photochemical reactions is difficult. Targeting complexes with electron deficient metal centers and strongly π and/or σ donors provides a sufficient starting point for designing complexes with LMCT excited states capable of photochemistry, yet these design principles are complex in practice. Molecular geometry, ligand donor ability, metal identity, and oxidation state all impact molecular orbital energetics, relative ordering of excited states, and even the metal vs. ligand character of excited states. In result, transition metal complexes that exhibit low-lying LMCT excited states and undergo photochemical reactions exhibit diverse structures, as they have found design constraints that balance each of the outlined criteria.

Motivated by the complexity of photosensitizer and photocatalyst design, we have chosen to briefly highlight trends observed for complexes with low-lying LMCT excited states and general precedence for engendering LMCT excited states through coordination complex design. While only some of these complexes have been employed for photochemical applications, understanding ways to systematically design complexes with low-lying LMCT excited states is a key first step in achieving widespread photochemical reactivity. Below, we discuss general ligand properties, then review trends within families of coordination complexes with the same d-electron configurations.

A variety of ligands are well known to support LMCT excited states, including π donating halides, oxos, sulfides, and alkoxy ligands, as well as σ-donating diphosphines, pyridinedipyrrolides, and *N*-heterocyclic carbenes.[18,20,22,33–54] However, in addition to classically categorized σ and π donors, other ligands typically perceived as π acceptors have also been reported to support LMCT excited states. For example, cyanide- and isocyanide-containing compounds are known to support low-lying LMCT excited states.[55–61] Furthermore, in a recent study polypyridyl nitrogen-based ligands, traditionally viewed as π-accepting aromatic ligands, were found to engage in bonding as π-donors when coordinated to first row transition metals.[62] This observation, in conjunction with other examples, showcases the diversity of ligands that are known to support

complexes with LMCT excited states. It also further underscores the opportunity to leverage TD-DFT to help identify and visualize the ligand-based orbitals that participate in LMCT transitions, and gain a deeper understanding of the ligand properties needed to support low energy LMCT excited states.[22,47,55,63–65]

The d electron configurations for complexes with LMCT excited states are also diverse. In particular, d^0 complexes are well known for low-lying LMCT excited states, resulting from their vacant metal orbitals which can easily be populated by filled ligand orbitals. When d orbitals are filled, d electrons are capable of participating in their own excitation processes, such as d–d transitions, metal-to-ligand charge transfer, and other metal-based charge transfer processes (select d configurations shown in **Figure 2**). For d^0 complexes, these competing transitions (and the resultant excited states) are absent, rationalizing their abundance within the field of LMCT excited states. Quintessential examples of low-lying LMCT excited states include d^0 complexes, such as vanadate, chromate, permanganate, and Group (IV) metallocenes.[23,26,64,66–73]

In addition to supporting low-energy LMCT transitions, the d^0 electronic configuration is also advantageous because the absence of d–d transitions eliminates a common pathway for excited state deactivation and simultaneously enables the opportunity for intersystem crossing of a singlet excited state to a triplet excited state — two qualities that are known to increase excited state lifetimes. However, despite these promising features, only a few examples of long-lived excited states from d^0 LMCT excited states have been reported, including pentamethylcyclopentadienyltantalum(V)-based complexes, tantalum(V) imido complexes, scandocene derivatives, and zirconium(IV) bis(pyrroyl)pyridine-based complexes, highlighting an opportunity for further growth within the field of LMCT.[46,47,74–78] Regardless, several d^0 complexes are known to promote photochemical reactions, several of which will be highlighted below.

Coordination complexes with other d electron configurations that have low energy LMCT excited states are also capable of promoting photochemical reactions. While d^0 complexes are by far the most common transition metal complex to exhibit low-lying LMCT excited states, the second most common electronic configuration is likely d^5, highlighted in **Figure 2**. For many d^5 complexes with low-lying LMCT excited states, strong σ donor ligands help deactivate ligand field states. In many cases, this strong σ donation results in low spin configurations, such as for iron(III) *N*-heterocyclic carbene complexes.[2,49] However, it is important to note that high spin configurations are also possible for d^5 complexes and can similarly facilitate photochemical reactions, as showcased by the visible light-induced homolysis of ferrioxalate. In addition to incorporating strong σ donors to destabilize ligand field states, another common design strategy is to access low spin configurations by employing second or third row transition metals, which exhibit larger ligand field splitting compared to first row counterparts. Recently, this low spin d^5 electronic configuration has been termed a "sweet spot" for designing complexes with LMCT excited states and has shown great promise in enabling photochemical reactions, several of which are highlighted herein.[2] Notably, however, low spin d^5 complexes have excited states with doublet character. As such, intersystem crossing is not accessible and these complexes often have short excited state lifetimes.

In addition to d^0 and d^5 electronic configurations, LMCT excited states are also possible from other electronic configurations. Complexes with lower d electron configurations (*i.e.,* d^1-d^4 electron configurations) are known to have LMCT transitions;[18,79–83] however, most of these known complexes, have low-lying d–d transitions that deactivate low-energy LMCT excited states and limit photochemistry from LMCT states. For example, $[Cr^{III}(ddpd)_2]^{3+}$ (ddpd = *N,N'*-dimethyl-*N,N'*-dipyridin-2-ylpyridine-2,6-diamine) and other complexes in the molecular ruby family have recently gained notoriety for their long-lived near-IR photoluminescence. However, it is important to note that this luminescence stems from intersystem crossing from metal-based or LMCT excited states to spin-flip (d–d excited) states, generating long-lived, spin-forbidden near-IR emissions.[80] Analogous emission has also recently been reported a Mn(IV) N-heterocyclic carbene complex.[53,80,81,84] One notable exception is of a homoleptic Mn(IV) complex with 2,6-diguanidylpyridine ligands which was recently reported to undergo excited state reductions from its low-energy ^{2}LMCT and ^{4}LMCT excited states.[65] Other photochemical applications from low energy LMCT excited states of d^1-d^4 complexes are quite rare, and if present result from anti-Kasha behavior.

LMCT excited states for complexes with higher electron d configurations (i.e., d^6-d^9) are also reported, and a few have been utilized as photocatalysts. Many of these complexes are comprised of first row transition metals with strong π and σ donors and notable examples include cobalamin, cobaloxime, tris(bipyridine)cobalt(III), bis(2,6-diguanidylpyridine)cobalt(III) complexes, copper(II) phenanthroline-based complexes, and a variety of metal halide complexes.[62,85–89] Several of these complexes, particularly metal halide complexes, have also gained traction as photoredox catalysts to drive a variety of organic transformations.[1,86,89,90,90,91,91–93] Like d^5 complexes, these electronic configurations enable a variety of d–d transitions and MLCT excited states, as illustrated in **Figure 2**.[1,19,62,94–98] Therefore, careful control of orbital energetics is required to preferentially enable low energy LMCT excited states.

Finally, it is worth noting that LMCT transitions are also accessible from lanthanide-based complexes, where LMCT transitions result in the population of low-lying f orbitals instead of d orbitals. While this topic will not be directly covered within this perspective article, several f-block metal complexes are known to facilitate low-energy LMCT excited states. Examples include cerium(IV) hexachloride, cerium(IV) carboxylates, cerium(IV) mixed-ligand guanidinate-amide complexes, ytterbocene complexes, europium(III) terpyridine-based complexes, among others.[99–104] Recent reports have also showcased their role in dictating the luminescent properties of f-block metal complexes and their utility in driving photoredox reactions via VLIH, illustrating analogous applications to their d-block brethren.[105–108]

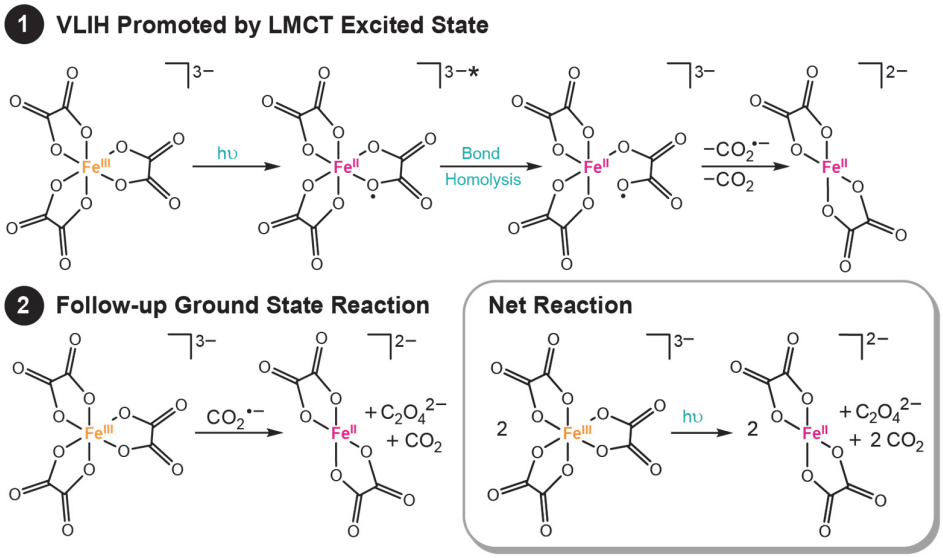

Figure 3. VLIH mechanism of ferrioxalate to form ferrous oxalate. Further decomposition of the $C_2O_4^{\bullet -}$ with a second equivalence of ferric oxalate yields an additional equivalence of ferrous oxalate and two equivalents of CO_2.

Collectively, these examples showcase the diversity of complexes known to support low energy LMCT excited states. d^0 complexes are well-known to promote low energy LMCT excited states, whereas d^1-d^9 complexes rely on a careful balance of metal identity, oxidation state, molecular geometry, and ligand sets to support low-lying LMCT transitions. Accessing photochemistry from these excited states is similarly complex and requires careful consideration of each of these criteria to enable desired photoreactivity. As such, we have chosen to briefly review a selection of coordination complexes with LMCT excited states and discuss the photochemical reactions that they promote. This selection aims to demonstrate the breadth of photochemistry accessible by LMCT excited states and provide perspectives on opportunities to drive photochemistry from LMCT excited states within a broader scope.

Photochemical Reactivity from LMCT Excited States

Transition metal complexes with LMCT excited states are known to undergo several types of photoreactions, including visible light-induced homolysis (VLIH), excited state electron transfer (ES-ET), and photoinduced chemical transformations.

I. Visible Light-Induced Homolysis

One of the most common photoreactions that transition metal complexes with LMCT excited states undergo is visible light-induced homolysis (VLIH). In VLIH reactions, homolysis of a metal-ligand bond is promoted by irradiation, producing a formally reduced metal center and oxidized ligand radical. While the net observed chemistry is bond homolysis of a metal-ligand bond, the chemistry is best thought of as a two-step process. First, light promotes intramolecular electron transfer (ET) from a coordinating ligand to a metal center, producing a formally reduced metal center and oxidized ligand radical. Second, the ligand radical dissociates. VLIH reactions are capable of forming a variety of reactive radical species, including carboxylate, halogen, and azide radicals, among others, and commonly initiate follow-up chemical reactions in the ground state. Common applications of VLIH include actinometry and photoredox catalysis.[1,21,92,97,98,109–111] Herein, we highlight two examples and discuss their mechanistic details.

Ferrioxalate

Potassium ferrioxalate (ferric oxalate, $K_3[Fe^{III}(C_2O_4)_3]$) is well-known for its use as a chemical actinometer, which enables the measurement of photon fluxes and quantum yields for a variety of applications. The photochemical reaction of ferrioxalate to produce ferrous oxalate was first reported by Allmand and Webb.[21] Its use as an actinometer was greatly expanded upon by Hatchard and Parker, whom extensively investigated ferrioxalate's quantum yields under a variety of conditions and enabled its widespread use across the field of photochemistry.[112,113] In a prototypical actinometry experiment, potassium ferrioxalate is dissolved in an acidic solution and photolyzed with light (ranging from 254 to ~550 nm), producing ferrous oxalate ($[Fe^{II}(C_2O_4)_2]^{2-}$).[112,113] This complex is then typically "developed" in excess phenanthroline (phen) within an acetate buffer to quantitatively yield $[Fe^{II}(phen)_3]^{2+}$ and ease quantum yield determination experiments, as the absorption profile of $[Fe^{II}(phen)_3]^{2+}$ is more readily resolved than that of ferrous oxalate.[113,114]

The photochemistry of ferrioxalate is promoted from the irradiation of a broad absorption centered at λ_{max} = 260 nm, spanning toward the red (to ~550 nm).[115] This feature exhibits a molar extinction coefficient of ~6000 $M^{-1}cm^{-1}$ consistent with a charge transfer excited state.[115] Further visualization of this

excited state was provided by Ogi et al., who showed through TD-DFT calculations that two ligands donate electron density to an iron d orbital, albeit the visualized transition is one of many that make up this absorption band.[116] Other natural transition orbitals are reported to have analogous LMCT character and the calculated UV-vis absorption spectrum constructed from these identified transitions is consistent with the experimental spectrum.[116] The broad absorption is ideal for actinometry experiments and further showcases the widespread utility of this compound.

Photochemical actinometry experiments exploit the LMCT excited state of ferrioxalate to drive reactivity that forms ferrous oxalate, CO_2, and oxalate, as summarized in **Figure 3**. Most commonly, a bond homolysis mechanism is used to rationalize this observed photochemical reactivity, where light promotes electron transfer from the oxalate ligand to the Fe center, followed by dissociation of an unstable oxalate radical anion ($C_2O_4^{\bullet -}$), see **Figure 3**.[115,117–119] Recent ultrafast time-resolved mid-IR spectroscopy experiments showed that the C–C bond of $C_2O_4^{\bullet -}$ rapidly cleaves to form CO_2 and $CO_2^{\bullet -}$, the latter is capable of thermally reducing another equivalent of ferrioxalate.[120] Complimentary time-resolved X-ray absorption and computational reports further support these claims.[116] Similar reactivity has been noted across a series of iron(III) carboxalato complexes.[121] This general photoreactivity showcases a potent route to form $CO_2^{\bullet -}$ and other potent radical anions.[117,121]

Nickel(III) Trihalide Complexes

Ni(III) trihalide complexes supported by chelating diphosphines ($Ni^{III}X_3(PP)$ where X = Cl or Br and PP = diphosphine) are known to photoeliminate halogen radicals through VLIH and are widely applied within the field of photoredox catalysis. These complexes exhibit broad absorption features across the visible spectrum, comprised primarily of LMCT transitions. Interestingly, higher energy LMCT excited states primarily drive this photochemistry, as supported by wavelength-dependent quantum yields.[19] Time-resolved X-ray diffraction (TR-XRD) measurements (photocrystallography) of a $Ni^{III}X_3PP$ species following irradiation with 365 nm light revealed that the apical Ni–X bond has photochemical lability.[19] TD-DFT calculations further rationalize these results, as low energy LMCT excited states primarily populate a Ni($3d_{x^2-y^2}$) antibonding orbital and higher energy LMCT excited states populate a Ni($3d_{z^2}$) antibonding orbital.[19,94] Therefore, LMCT transitions with Ni($3d_{z^2}$) acceptor orbitals were determined to drive the photochemistry observed via TR-XRD with high energy irradiation.

Nocera's original report of $Ni^{III}X_3(PP)$ photochemistry investigated the stabilizing effect of the 1,2-bis(diphenylphosphino)ethane ligand (dppe) on the released halogen radical (**Figure 4**). Within < 40 ns, transient absorption measurements of $NiCl_3$(dppe) revealed a species with absorption maxima at 366 nm and 525 nm, assigned to an arene-to-chlorine atom charge-transfer adduct.[19] Analogous signals have been observed across a variety of aryl-containing $NiX_3(PP)$ analogues and support that the photogenerated

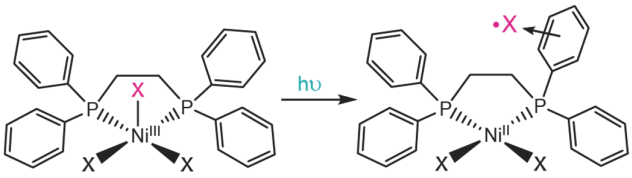

Figure 4. Irradiation $Ni^{III}X_3$(dppe), shown here, and other $Ni^{III}X_3PP$ complexes results in VLIH of the Ni-X bond, where the resulting halogen radical is stabilized by arene substituents on the diphosphine ligand.

chlorine radical is stabilized on the aryl substituents for up to several microseconds depending on the diphosphine substituents.[19,94] Furthermore, the aryl groups significantly increase the quantum yield for halogen release with aliphatic groups producing quantum yields of 20% and aryl-containing groups exhibiting quantum yields up to 96%.

While many complexes have been reported to liberate halogen atoms following photoexcitation, including many metal complexes with LMCT excited states, these nickel(III) trihalide complexes incorporate an important design principle not described in other systems – halide radical stabilizing substituents in the secondary coordination sphere. This finding suggests that simple manipulation of ligand properties can impart stabilizing interactions with halogen radicals and improve photochemical outcomes. These interactions tune the quantum yields of halogen radical production and increase the lifetime of these halogen radical intermediates – parameters critical for dictating the efficiency of photoredox catalysis reactions.

II. Excited State Electron Transfer

One of the most fundamental photochemical reactions for LMCT excited states is excited state electron transfer (ES-ET). Excited states, regardless of their character, are inherently better reductants and oxidants than their ground state counterparts, as the chemical potential generated in the excited state promotes reduction and oxidation at milder potentials. Due to the higher chemical potential of the excited state, promoted electrons (holes) can more easily transfer to (from) quenching substrates. The potency of these excited state reduction potentials is dictated by two factors: the ground state reduction potential ($E^{\circ\prime}$) and the energy stored in the excited state (ΔG_{ES}).[122] This relationship is summarized in Eq 1-2, where $E^{\circ\prime}(M^{(n+1)/n})$ is the reduction potential corresponding to the oxidation of the photosensitizer and $E^{\circ\prime}(M^{n/(n-1)})$ is the reduction potential for the reduction of the photosensitizer. For each case, these ground state reduction potentials are modified by ΔG_{ES} to yield the excited state reduction potentials relevant for photooxidative and photoreductive processes (Eq 1 and 2, respectively, where ΔG_{ES} is in units of eV).[122]

$$E^{\circ\prime}(M^{(n+1)/n*}) = E^{\circ\prime}(M^{(n+1)/n}) - \Delta G_{ES} \quad (1)$$

$$E^{\circ\prime}(M^{n*/(n-1)}) = E^{\circ\prime}(M^{n*/(n-1)}) + \Delta G_{ES} \quad (2)$$

While thermodynamics dictate the reducing and oxidizing power of excited states, kinetic factors also drive the accessibility of ES-ET reactions. In many cases, the lifetime of the excited state dictates whether or not ES-ET can occur by

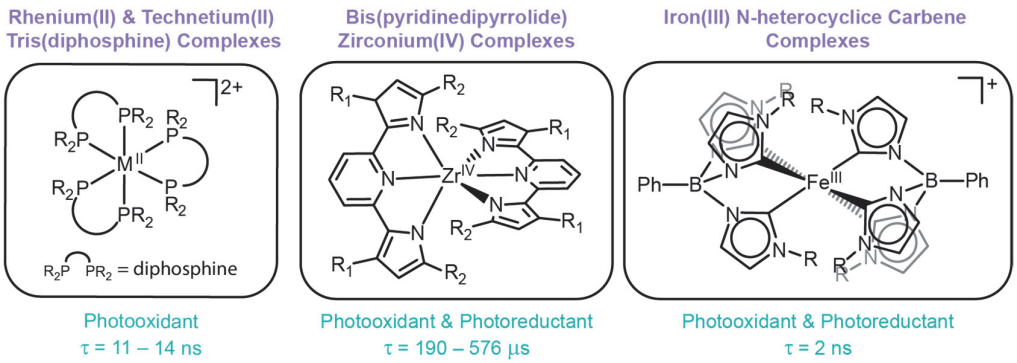

Figure 5. Structures of three classes of compounds known to facilitate ES-ET reactions (where M = Re or Tc). A summary of their role as photooxidants and/or photoreductants are included, alongside their respective excited state lifetimes.

dynamic quenching before the excited state relaxes via radiative or non-radiative pathways. If an excited state is too short-lived, the photosensitizer is unable to accept (donate) an electron from (to) a substrate. Furthermore, the stability of the oxidized (reduced) photosensitizer is also essential to drive photocatalytic systems with photosensitizing compounds. If ES-ET results in a chemically unstable photosensitizer product, degradation reactions will inhibit desired reactivity, reducing quantum yields, and preventing photosensitizer recyclability.[5] While ES-ET is theoretically possible from all LMCT excited states, some LMCT excited states exhibit sub-nanosecond lifetimes at room temperature (including those that cannot undergo inter-system crossing, such as d^5 species with doublet ground states) and/or promote metal complex degradation via pathways like VLIH (see above), hindering their widespread use as photosensitizers. While extended reaction times and higher photon flux can enable photosensitization in some cases, the utility of these short-lived excited states is still limited compared to other state-of-the-art photosensitizers, like $[Ru(bpy)_3]^{2+}$. Despite these limitations, a handful of LMCT-based photosensitizers are known, including rhenium(II) tris(diphosphine), zirconium(IV) bis(pyrrolyl)pyridine, iron(III) N-heterocyclic carbene complexes (**Figure 5**).[45,47,123]

Rhenium(II) Tris(diphosphine) Complexes

$[Re(dmpe)_3]^{2+}$ (dmpe = 1,2-bis(dimethylphosphino)ethane) exhibits room-temperature luminescence[20] with a nanosecond lifetime (11 – 14 ns depending on solvent) sufficient for bimolecular electron transfer.[42,45] Computational studies identified a ^{2}LMCT excited state, consistent with fast, spin-allowed excited state decay. Re and Tc derivatives supported by other chelating diphosphine ligands also exhibit similar photochemical properties.[20,42,44,45,63] Holistically, this class of d^5 compounds exhibits highly oxidizing excited states with $E^{o\prime}(M^{II*/I})$ values ranging from 2.06 to 2.63 V vs. Ag/Ag^+.[42,45] These complexes are more oxidizing than $[Ru(bpy)_3]^{2+}$ and can oxidize traditionally recalcitrant substrates, like anisole, toluene, and chloride ions.[42,45,122] While their use as photooxidants is impressive, their ability to act as photoreductants is quite limited, a result of ligand dissociation upon oxidization. Cyclic voltammograms of rhenium(II) tris(diphosphine) complexes show an irreversible $Re^{III/II}$ redox couple, consistent with chemical reactivity upon oxidation.[45] In addition, several mechanistic studies have proposed solvent-assisted dissociation mechanisms upon oxidation of Re^{II}, resulting in the loss of one diphosphine ligand and coordination of solvent (S) to produce $[Re(dmpe)_2S_2]^{3+}$.[41,45] While unfortunate, this oxidative instability is unsurprising, owing to the electronic configuration of these Re^{III} species, and will likely be difficult to overcome for this class of compounds.[20,41,45,124]

Thorough studies of rhenium(II) and technetium(II) diphosphine complexes have illustrated their predilection for undergoing excited state reductions. However, their propensity to undergo degradation upon (photo)oxidation exposes their primary weakness: ligand loss. Unfortunately, this characteristic is not isolated to rhenium(II) and technetium(II) tris(diphosphine) complexes, but instead is a recurring theme within the field of LMCT photochemistry. In this specific case, ligand flexibility permits solvent-assisted photodissociation of a diphosphine ligand and prevents reversible excited state oxidations to drive photoreduction reactions.[20,41,45,124] Other examples of photoinstability are also well-reported, either via VLIH reactions or dissociation pathways, typically from monodentate ligands.[1,2,55,92] This predisposition emphasizes the pervasive need to identify and/or design ligand scaffolds that facilitate oxidative stability and prevent dissociative pathways to enable photosensitizing applications.

Zirconium Bis(pyrroyl)pyridine Complexes

Bis(pyridinedipyrrolide)zirconium(IV) complexes, $Zr(PDP)_2$, first reported by the Milsmann group, exhibit exceptionally long emission lifetimes ranging from 190 – 576 μs at room temperature.[22,47,125] These d^0 complexes are one of the first examples of an earth abundant metal-containing photosensitizer with lifetimes comparable to complexes with MLCT excited states.[13,17,126] Very few complexes with emissive LMCT excited states are known and of those, most are short-lived and/or only emissive at low temperatures.[20,49,50,56,66,70,74,76,78,86,127–129] Computational studies propose their low energy emission stems from a mixed ^{3}LMCT/^{3}LLCT excited state where the ground state is entirely ligand-based and the excited state exhibits mixed metal and ligand character, consistent with the experimentally observed long-lived excited state.[22,47] Interestingly, spectroscopic studies further deciphered the origin of this photoluminescence and found $Zr(PDP)_2$ complexes exhibit thermally activated delayed

fluorescence whereupon reversible intersystem crossing enables emission from both the singlet and triplet states across a range of temperatures.[77] Manipulating the substituents on the PDP ligands affects the absorption profile minimally, but enables moderate electronic tuning. Across seven complexes, ground state and excited state reduction potentials were tuned by almost 600 mV, as absorption and emission profiles remained constant.[125] Interestingly, the LMCT character of the excited state varies with substituent, ranging from 25% to 40%, where the remainder exhibits LLCT character.[22,47,125]

These complexes have been employed as photosensitizers across a variety of photocatalytic reactions, including dehalogenation, trifluoromethylation of electron-rich arenes, and atom transfer radical addition reactions. In these reactions, $Zr(PDP)_2$ undergoes ES-ET to (from) a substrate and follow-up reactivity of the activated substrate in the ground state yields targeted products.[22,47,77,125] Addition of mild reductants (or oxidants) enables regeneration of $Zr(PDP)_2$ and promotes catalytic turnover. Interestingly, the PDP ligands not only serve to direct electronics and tune the potency of excited state reduction potentials, but also to stabilize the complex itself. Early studies showed the $Zr(^{Me}PDP^{Ph})_2$ derivative ($^{Me}PDP^{Ph}$ = 2,6-bis(5-methyl-3-phenyl-1H-pyrrol-2-yl)pyridine) easily hydrolyzes at its basic pyrrolide nitrogens.[77] Furthermore, while this complex exhibits reversible ground state reductions, the oxidation of $Zr(^{Me}PDP^{Ph})_2$ is irreversible (reminiscent of rhenium(II) tris(diphosphine) complexes).[22] As such, excited state reduction of $Zr(^{Me}PDP^{Ph})_2$ to $[Zr(^{Me}PDP^{Ph})_2]^-$ was accessible with a $E^{o\prime}([Zr]^{0*/-})$ = –0.07 V vs. $Fc^{+/0}$, but excited state oxidation to form $[Zr(^{Me}PDP^{Ph})_2]^+$ was associated with decomposition and prevented its use as a photoreductant.[22] Interestingly, slight modification of this ligand, where methyl groups on the pyrrole rings were replaced with mesityl groups (denoted $Zr(^{Mes}PDP^{Ph})_2$), resulted in a complex that was resistant to hydrolysis and exhibited greater thermal and oxidative stabilities. Unlike its predecessors, $Zr(^{Mes}PDP^{Ph})_2$ exhibits two reversible redox features and, as such, both oxidative and reductive quenching pathways for this class of compounds were reported for the first time ($E^{o\prime}([Zr]^{+/0*})$ = –1.41 V and $E^{o\prime}([Zr]^{0*/-})$ = –0.31 V vs $Fc^{+/0}$, respectively).[77]

$Zr(PDP)_2$ complexes are robust and powerful photoredox reagents that promote oxidation and reduction of substrates from their excited states. The absence of d electrons prevents deleterious deactivation pathways from ligand field states to support long-lived LMCT excited states. First generation complexes experienced oxidative instability, but synthetic tuning enabled a second generation of robust $Zr(PDP)_2$ complexes capable of supporting stable excited state charge transfer products. This example showcases the importance of ligand design in enabling photostable LMCT excited states capable of undergoing ES-ET and serves as a direct testament for targeting robust oxidizable ligands to support LMCT excited states.

Iron N-heterocyclic Carbene Complexes

A class of iron(III) homoleptic complexes employing facial tridentate scorpionate ligands, $[Fe^{III}(phtmeimb)_2]^+$ (phtmeimb = phenyl[tris(3-methylimidazol-1-ylidene)]borate), has recently been reported to exhibit nanosecond lifetimes from LMCT excited states.[49] These Fe(III) complexes exhibit exceptionally long-lived excited states for both iron-based complexes and doublet excited states. In comparison, their record-breaking predecessor, an Fe^{III} complex with bidentate N-heterocyclic carbene ligands, $[Fe(btz)_3]^{2+}$ (btz = 3,3′-dimethyl-1,1′-bis(p-tolyl)-4,4′-bis(1,2,3-triazol-5-ylidene), exhibits a 100 ps LMCT lifetime.[2,49] In both classes of iron(III) N-heterocyclic carbene complexes, the strongly σ-donating N-heterocyclic carbene ligands are sufficient to raise metal-centered states above the ^{2}LMCT excited state and enable unprecedented long photoluminescence lifetimes for an iron complex.[49,50,130]

Due to the nanosecond timescales required to access bimolecular reactions at modest substrate concentrations and reaction length, only $[Fe^{III}(phtmeimb)_2]^+$ complexes have exhibited ES-ET reactivity. In fact, $[Fe^{III}(phtmeimb)_2]^+$ was the first known iron complex with a charge-transfer excited state to undergo excited state quenching.[49,130] This complex is both potent as a photo-oxidant and photoreductant ($E^{o\prime}([Fe]^{IV/III*})$ = –1.9 V and $E^{o\prime}([Fe]^{III*/II})$ = 1.0 V vs. $Fc^{+/0}$). Since the seminal report, several studies have further investigated this class of compounds for ES-ET reactions, including photocatalytic dehalogenation reactions.[49,123,131] Follow-up synthetic studies by Wärnmark and coworkers have attempted to further tune the excited state reduction potentials and identify structure-(photo)functional relationships through modulation of the 4-position of the phenyl group within the scorpionate ligand with electron-donating and electron-withdrawing groups. However, the excited state reduction potentials and lifetimes were extremely similar, suggesting that the modification at this position was not impactful in modulating the excited state.[130] While this observation did not provide synthetic strategies for improving its photophysical properties, it does showcase that the 4 position of the scorpionate's phenyl substituent can be exploited as an attachment point to construct molecular or hybrid assemblies, a strategy commonly invoked for photosensitizing architectures.

The photostability of substituted $[Fe(phtmeim)_2]^+$ complexes have also been investigated within a visible-light-mediated dehalogenation catalysis reaction of 4-bromobenzyl-2-chloro-2-phenylacetate. $[Fe(phtmeim)_2]^+$ was employed as a reductive quencher to facilitate the dehalogenation reaction of 4-bromobenzyl-2-chloro-2-phenylacetate and compared to a prototypically employed photosensitizer, $[Ru(bpy)_3]^{2+}$. Significant ligand loss was observed for $[Ru(bpy)_3]^{2+}$, whereas $[Fe(phtmeim)_2]^+$ showed no noticeable degradation.[130] Collectively, these studies highlight the photostability of a transition metal complex that exhibits a lifetime on the nanosecond timescale, a tailorable ligand scaffold, and photochemical stability – three characteristics that have been historically difficult to simultaneously achieve for complexes that exhibit LMCT excited states. Therefore, future studies within the field of LMCT should greatly consider the design features implemented within this scaffold to inspire next-generation photosensitizing and photocatalytic systems.

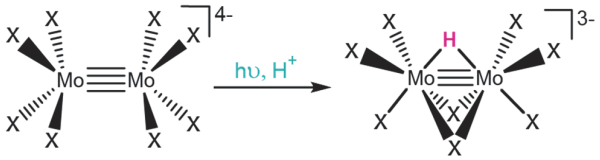

Figure 6. Excited state protonation of $[Mo_2X_8]^{4-}$ yields $[Mo_2(\mu\text{-}H)(\mu\text{-}X)_2(X)_6]^{3-}$.

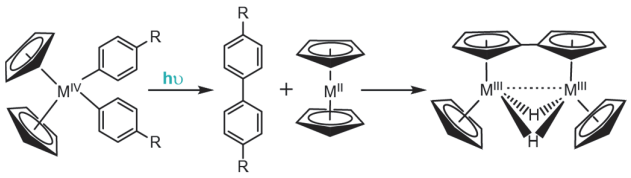

Figure 7. Irradiation of Cp_2MR_2 complexes (R = Ar) results in photo-induced reductive elimination to form biphenyl derivatives.

III. Photochemical Transformations

VLIH and ES-ET reactions from LMCT excited states enable routes to generate reactive species, such as electron rich radicals or oxidized/reduced analytes. However, a less explored strategy to exploit LMCT excited states is to promote chemical transformations at the light absorber itself. Enabling these reactions is essential to access photocatalytic transformations, where the metal center can bind substrates, chemically transform them into value-added products, and release these products to enable catalytic turnover. Two such reactions, excited state protonation and photoinduced reductive elimination, are highlighted herein. While simple in nature, these proton transfer and reductive elimination steps are central to a variety of catalytic reactions and when coupled to light absorption could revolutionize our approaches to chemical synthesis.

Excited State Protonation of Octahalodimolybdates

While excited state electron transfer is well known for several complexes that have LMCT excited states, there is currently only one known example of excited state proton transfer involving a LMCT excited state. Upon UV irradiation, octahalodimolybdates, $[Mo_2X_8]^{4-}$ where X = Cl or Br, are known to undergo excited state protonation in dilute mineral acids. Growth of a UV-vis absorption feature at 415 nm confirmed the formation of a bridging metal hydride, $[Mo_2(\mu\text{-}H)(\mu\text{-}X)_2(X)_6]^{3-}$ (**Figure 6**).[18] Over time, this metal hydride gradually reacts in aqueous acids to yield an aquated molybdenum species and stoichiometric equivalence of H_2, as supported by synthetic isolation of the hydride intermediate and associated isotopic labelling studies.[18,132,133]

While excited state protonation and associated ground state reactivity was observed for $[Mo_2X_8]^{4-}$, it is important to note the conditions of this photolysis experiment. Under dark conditions, ground state protonation for $[Mo_2X_8]^{4-}$ is known, where reaction kinetics to form $[Mo_2(\mu\text{-}H)(\mu\text{-}X)_2(X)_6]^{3-}$ are sluggish at low mineral acid concentrations and fast at high concentrations. Therefore, photolytic conditions employed low acid concentrations to minimize competitive protonation in the ground state, due to the irreversibility of these photoreactions. By irradiating aqueous solutions of $[Mo_2X_8]^{4-}$ with UV light, the formation of $[Mo_2(\mu\text{-}H)(\mu\text{-}X)_2(X)_6]^{3-}$ occurred much faster than in the dark, suggesting a new light-driven mechanism was operable.[18] These observations are consistent with the formation of an excited state that is more basic than its ground state analogue and the more facile generation of $[Mo_2(\mu\text{-}H)(\mu\text{-}X)_2(X)_6]^{3-}$ with UV irradiation.

Gray and coworkers attributed this change in basicity to the nature of the irradiated state.[18] They assign an UV absorbance feature at 270 nm (320 nm) for $[Mo_2Cl_8]^{4-}$ ($[Mo_2Br_8]^{4-}$) as a ligand-to-metal charge transfer excited state, where halide (π) ligand orbitals populate a Mo-Mo δ* orbital.[18,134] This electronic transition significantly shifts the electron density toward the Mo-Mo centers and increases their relative basicity in the excited state.[134] Surprisingly, photochemistry from this charge transfer excited state disobeys Kasha's rule, as photochemical $[Mo_2(\mu\text{-}H)(\mu\text{-}X)_2(X)_6]^{3-}$ formation was only observed upon irradiation of the high energy LMCT features, not at optical features observed at lower energies. Control photolytic studies showed no photochemical $[Mo_2(\mu\text{-}H)(\mu\text{-}X)_2(X)_6]^{3-}$ formation from lower energy δ → δ* transitions (centered at 510 nm and 518 nm for $[Mo_2Cl_8]^{4-}$ and $[Mo_2Br_8]^{4-}$, respectively).[18] This uncommon photochemical occurrence was rationalized by slow internal conversion rates to metal-centered orbitals. While several follow-up studies have further investigated these complexes (e.g., ground state protonation and electronic structure via TD-DFT),[135,136] many questions still remain, including the geometry of the orbitals involved in the excited state protonation and exact mechanism of protonation to form the metal hydride (i.e., protonation to a bridging or terminal position). This example illustrates the unique reactivity of octahalodimolybdates in driving excited state protonation by LMCT and further showcases the promise of these excited states to enable fundamental photochemical reactivity, like transition metal hydride formation, and pursuit of more complex photocatalytic schemes.

Photoinduced Reductive Elimination of Titanium- and Zirconium-based Complexes

Group IV diarylmetallocene complexes are well known for their photoinduced reductive eliminations. This photochemical reaction was first reported by Erker in 1977, where irradiation of diarylzirconocenes with a mercury bulb resulted in quantitative isolation of biphenyl derivatives (**Figure 7**, see concept below).[23] Further inspection of this system noted a bright purple bridging dihydride fulvalene complex (and known dimerization product of zirconocene), supporting a photoinduced reductive elimination mechanism.[137] Since this first reaction was reported, several titanium analogues that produce comparable C–C coupled photoproducts have also been reported.[68,72,138–142] Detailed mechanistic studies have revealed that these complexes preferentially undergo a reductive coupling step to yield C–C bonds over M–C bond

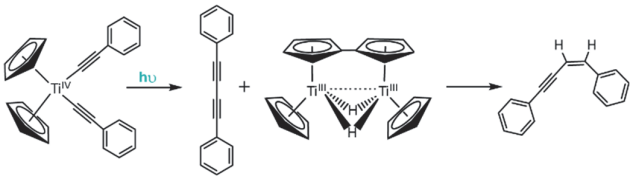

Figure 8. Irradiation of arylalkynl titanocene complexes results in photo-induced reductive elimination to form an enyne product.

homolysis, whereas other Cp_2MR_2 type complexes (such as dialkyltitanocenes and dicarbonyltitanocenes) and are known to selectively undergo M–C bond homolysis upon irradiation.[67,142,143]

Since these original reports, the photophysics and photochemistry of Cp_2TiR_2 complexes (where R = arylethynyl ligands) have been extensively studied.[140–142] Wagenknecht and coworkers employed TD-DFT studies to computationally rationalize the observed photoreactivity and discovered the lowest energy transition for these complexes is a LMCT transition dominated by donation from the arylalkynyl ligands to the Ti $d_{z^2-y^2}$ orbital.[140] Photo-induced population of the Ti $d_{z^2-y^2}$ antibonding orbital weakens the bond between the Ti metal and arylalkynyl π orbitals and facilitates the experimentally observed reductive elimination of the arylalkynyl ligands. Interestingly, for this class of Cp_2TiR_2 compounds, the major product is not a diyne (the anticipated reductive coupling product), but instead an enyne. Control studies revealed the resulting titanocene by-product is non-innocent following the photo-induced reductive elimination. Accounts from Brintzinger and Bercaw show that titanocene is not stable and readily undergoes dimerization to yield a strongly reducing, bridging dihydride fulvalene complex (**Figure 8**).[144] Upon formation of the diyne, it is proposed to undergo rapid reduction to the enyne by the fulvalene complex either through a stepwise or concerted pathway, and has since been shown to occur across several synthetic derivatives.[138,140,141]

Further derivatization of these $CpTiR_2$ complexes supports that the LMCT excited state is responsible for driving the reductive photochemistry observed. When ferrocene moieties are appended to the alkynyl ligands of Ti, the lowest energy excited state exhibits metal-to-metal charge transfer (MMCT) character (instead of LMCT character), as the donor orbitals are primarily localized on the ferrocene moiety. As a result, this complex does not undergo photoinduced reductive elimination of its arylalkynyl ligands.[141] These examples support the assignment that photoinduced reductive elimination from Cp_2TiR_2 and Cp_2ZrR_2 is promoted by LMCT.

While many accounts report the photoreductive elimination of Cp_2MR_2 complexes as decomposition pathways, Chirik and coworkers describe the utility in harnessing this reactivity to access a reactive intermediate capable of activating N_2.[68] UV irradiation of $[(\eta^5\text{-}C_5Me_4H)_2Zr(Tol)_2]$ (Tol = 4-Me-C_6H_4, depicted in **Figure 9A**) under N_2 atmosphere resulted in quantitative conversion to 4,4'-dimethylbiphenyl and $[\{(\eta^5\text{-}C_5Me_4H)_2Zr\}_2(\mu_2,\eta^2,\eta^2\text{-}N_2)]$, a complex known to undergo hydrogenation and CO-induced N_2 cleavage.[68,145] Carbon monoxide and bis(trimethylsilyl)acetylene can similarly be

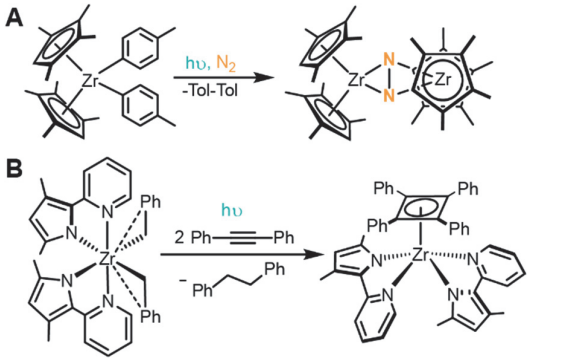

Figure 95. Summary of reactions for A) $[(\eta^5\text{-}C_5Me_4H)_2Zr(Tol)_2]$ and B) $(^{Me}PMP^{Me})_2ZrBn_2$.

trapped by this reactive synthon to form $[(\eta^5\text{-}C_5Me_4H)_2Zr(CO)_2]$ or $[(\eta^5\text{-}C_5Me_4H)_2Zr(\eta^2\text{-}Me_3SiCCSiMe_3)]$, respectively. Detailed mechanistic studies support this photoreaction follows a photoinduced unimolecular, two-electron reductive elimination to produce 4,4'-dimethylbiphenyl and $[(\eta^5\text{-}C_5Me_4H)_2Zr]$. The resulting 4,4'-dimethylbiphenyl photoproduct then likely associates to $[(\eta^5\text{-}C_5Me_4H)_2Zr]$, forming a stabilizing Zr-arene interaction, and enabling facile displacement by strong π donors. In the absence of π donors, like N_2, these Zr-arene complexes react further with the biphenyl photoproducts or aromatic hydrocarbon solvents via oxidative addition of the C-H bond to stabilize the undercoordinated metal center.[68]

The Milsmann group recently reported a similar photoinduced reductive elimination from $(^{Me}PMP^{Me})_2ZrBn_2$ ($^{Me}PMP^{Me}$ = 3,5-dimethyl-2-(2-pyridyl)pyrrol-ide and Bn = benzyl), illustrated in **Figure 9B**.[146] Upon irradiation to populate a LMCT excited state, this complex releases an equivalent of 4,4'-biphenyl as the only byproduct, akin to the reactivity observed in Cp_2MR_2 complexes described above. Interestingly, in the presence of diphenylacetylene, the resulting $(^{Me}PMP^{Me})_2Zr$ species was shown to form a rare η^4-cyclobutadienyl zirconium complex, $(^{Me}PMP^{Me})_2Zr(\eta^4\text{-}C_4Ph_4)$.[146] Such reactivity is reminiscent of Chirik's work,[68] as it showcases the stabilizing effect of a π donating ligand which binds to the Zr center following photoinduced reductive elimination. However, unlike the prototypical Cp_2MR_2 case, mechanistic studies within this work suggest that $(^{Me}PMP^{Me})_2ZrBn_2$ does not undergo concerted reductive elimination but instead follows a stepwise pathway, where it is proposed that Zr–C bond homolysis occurs to liberate a benzyl radical and accompanying Zr^{III} intermediate.[146] Subsequent ground state reactivity yields the observed 4,4'-biphenyl products, although the mechanistic details are still under investigation. This work showcases the intricacies of photoinduced reductive elimination steps. In each of these highlighted examples, similar reactions occur, yet their mechanistic details and accessible follow-up reactivity are different. This known disparity emphasizes the fundamental need to continue exploring the operative mechanisms for photochemical transformations promoted by LMCT.

Conclusions and Outlook

While LMCT excited states once received a forlorn reputation of instability and degradation, their redemption is underway. Over the past several decades, a range of reactivity has been seen for complexes with LMCT excited states, including photoinduced bond homolysis, excited state electron transfer, excited state proton transfer, and photoinduced reductive eliminations. This diverse reactivity offers a wide variety of opportunities to leverage the energy stored in excited states for complex, energy-intensive transformations and enable new photochemical and photocatalytic reactions with broad applications. Some examples have already achieved widespread notoriety, such as ferrioxalate with its widespread use as a chemical actinometer and halogen radical-generating complexes with their roles in photoredox catalysis. However, a variety of other photoreactions are known and the applications for these reactions have not been realized.

Challenges in the widespread adoption of LMCT-based photocatalysts and photosensitizers primarily stem from the absence of design principles for complexes with LMCT excited states. The structures of these LMCT-containing metal complexes are typically disparate and difficult to rationalize, making it difficult to design new photosensitizers and photocatalysts for niche applications. Some ligands are well known to support LMCT excited states, such as oxos and halides, whereas many other ligand scaffolds can facilitate a variety of charge transfer processes depending on the metal center identity, metal oxidation, and coordination geometry. As such, it is important to consider what factors are important in designing complexes to facilitate LMCT, but simultaneously consider the desired applications of these complexes for designing systems from the top-down.

First, the metal center identity, oxidation state, and coordination geometry are key to enabling LMCT excited states. Complexes must exhibit electron deficient metal centers that can easily be reduced upon photoexcitation. As a result, complexes with LMCT excited states are often d^0 and d^5, as their low energy t_{2g} orbitals are fully or partially unfilled. Other examples with higher d electron configurations, such as d^7 Ni^{III} and d^9 Cu^{II}, are typically supported by strongly σ-donating ligands which lower e_{2g} orbitals sufficiently to enable LMCT. However, in addition to preferentially tailoring these excited states to promote photochemistry, additional factors must also be considered. For example, d electron configurations are extremely important in dictating accessible photoproducts and photocatalytic intermediates generated from follow-up ground state reactivity. Photosensitizers must exhibit stability in their singly reduced and oxidized forms to enable turnover in photoredox catalytic reactions. Furthermore, if more complex photochemical transformations, like ES-PT and photoinduced reductive elimination reactions, are integrated into photocatalytic architectures, additional oxidation states must be accessed, as both processes result in oxidation states that decrease/increase by two, respectively. In addition to d electron configuration, metal identity and oxidation state also impacts ground state reduction potentials, and in turn excited state reduction potentials, enabling yet another synthetic variable to modulate photochemical reactivity. Absorption profiles and excitation energies of LMCT excited states may similarly change, allowing access to a breadth of photochemical applications.

The geometry of the orbitals that facilitate LMCT must also be considered. For photoinduced bond homolysis reactions, studies showed that charge transfer to a d_{z^2} orbital liberates an apical ligand due to perturbation of a σ-interaction in the excited state. However, this observation is extremely dependent on the geometry of the complex, its d-orbital splitting, orientation of the coordinating ligands, and energy of the incident photon. For applications targeting photoinduced bond homolysis, complexes that facilitate population of a d_{z^2} orbital would be more attractive and rationalizes the commonality of d^7 and d^8 complexes in facilitating photoinduced bond homolysis of apical ligands (as d_{z^2} orbitals are common SOMOs/LUMOs for these complexes). The metal complex geometry must also be considered for photocatalytic applications, as substrate binding to a metal is likely required. Therefore, complexes must either 1) exhibit an open coordination site in the ground state or 2) generate an open coordination site upon photoexcitation.

Finding a balance between each of these design criteria is critical for enabling more complex photochemical and photocatalytic reactions. In many cases outlined herein, the transition metal complexes with known photochemistry from LMCT excited states were studied via TD-DFT to rationalize the orbitals involved in the electronic transitions. While many of these studies retroactively determine the nature of the excited state, the converse approach is also feasible. TD-DFT calculations can provide essential predictive power in understanding a complex's electronic structure, specifically the ordering of excited states and orbital character, without synthesis or experiment. These calculations are especially useful when targeting unexplored and/or complex photochemical reactions, where TD-DFT calculations can expedite the design of complexes that will exhibit low-lying LMCT transitions and exhibit electronic structure that promote photochemical reactivity of interest. As such, TD-DFT calculations should be added to every chemist's toolbox prior to designing novel complexes with LMCT excited states and targeting specific photochemistry from those states.

In addition to tailoring the metal center identity, ligand scaffolds are also critical for dictating the reactivity of LMCT excited states. Complexes with LMCT excited states must exhibit oxidizable ligands, as they transfer electron density from ligands to the metal center upon irradiation. However, this irradiation may result in bond homolysis or reductive elimination. For some applications, this photoreactivity is advantageous. For other applications, like excited state electron transfer reactions, this reactivity is deleterious. In these cases, stable chelating ligands that donate electron density in the excited state should be targeted. However, it is important to note that not all chelating ligands are stable, as highlighted by the chemical actinometer ferrioxalate which undergoes bond homolysis and due to the instability of the carboxylate radical anion, and further decomposes. Similarly, diphosphines are

known to dissociate in rhenium(II) tris(diphosphine) complexes. Therefore, chelating ligand scaffolds that are donating, oxidizable, and stable are required to enable routes to photostabilize metal complexes.

Finally, the excited state lifetime and reaction quantum yields must be considered. Many coordination complexes with LMCT excited states are known to have short-lived excited states, often due to the lack of accessible intersystem crossing to long-lived excited states and/or fast deactivation by metal-centered states, as in the case of d^5 complexes with doublet ground and excited states. Short excited state lifetimes can limit bimolecular reactivity, such as excited state electron transfer and proton transfer reactions, where excited molecules must diffuse to their co-reactants. Conversely, intermolecular processes, such as photo-induced bond homolysis and reductive elimination reactions, are not limited by diffusion. Instead, these reactions typically occur on the femtosecond to picosecond timescales, rationalizing their proclivity within the reactivity arena of LMCT excited states. However, it is important to note that while these reactions occur on a fast timescale, the lifetime of these excited states is still important. Many of these reactions are proposed to occur on the vibrational timescale, such that if the excited state is longer-lived, a higher probability of a successful photoreaction is anticipated.

Overall, the design principles presented above must harmonize to enable the orchestration of complex photochemical reactions from LMCT excited states. Metal centers and their coordinating ligands must delicately balance one another to foster molecular geometries and electronic structures that enable low-lying LMCT excited states. From these excited states, a wealth of photochemical reactions are possible. Common photochemical examples include VLIH, ES-ET, ES-PT, and photoinduced reductive eliminations, but many other chemical transformations could also be envisioned. Driven by these prospects, and the guiding synthetic design principles outlined herein, complexes with low energy LMCT excited states are poised to overcome their proposed shortcomings and enable a new era of LMCT-driven photochemistry.

Conflicts of interest

There are no conflicts to declare.

Acknowledgements

This work was supported by the National Science Foundation (CHE-1954868). A.M.M. acknowledges support from the Department of Defense through the National Defense Science & Engineering Graduate (NDSEG) Fellowship Program.

Notes and references

1 Juliá, F. Ligand-to-Metal Charge Transfer (LMCT) Photochemistry at 3d-Metal Complexes: An Emerging Tool for Sustainable Organic Synthesis. *ChemCatChem* **2022**, *14* (19), e202200916. https://doi.org/10.1002/cctc.202200916.

2 Chábera, P.; Lindh, L.; Rosemann, N. W.; Prakash, O.; Uhlig, J.; Yartsev, A.; Wärnmark, K.; Sundström, V.; Persson, P. Photofunctionality of Iron(III) N-Heterocyclic Carbenes and Related D5 Transition Metal Complexes. *Coord. Chem. Rev.* **2021**, *426*, 213517. https://doi.org/10.1016/j.ccr.2020.213517.

3 Li, C.; Kong, X. Y.; Tan, Z. H.; Yang, C. T.; Soo, H. S. Emergence of Ligand-to-Metal Charge Transfer in Homogeneous Photocatalysis and Photosensitization. *Chem. Phys. Rev.* **2022**, *3* (2), 021303. https://doi.org/10.1063/5.0086718.

4 Wenger, O. S. Photoactive Complexes with Earth-Abundant Metals. *J. Am. Chem. Soc.* **2018**, *140* (42), 13522–13533. https://doi.org/10.1021/jacs.8b08822.

5 Arias-Rotondo, D. M.; McCusker, J. K. The Photophysics of Photoredox Catalysis: A Roadmap for Catalyst Design. *Chem. Soc. Rev.* **2016**, *45* (21), 5803–5820. https://doi.org/10.1039/C6CS00526H.

6 Scaltrito, D. V.; Thompson, D. W.; O'Callaghan, J. A.; Meyer, G. J. MLCT Excited States of Cuprous Bis-Phenanthroline Coordination Compounds. *Coord. Chem. Rev.* **2000**, *208* (1), 243–266. https://doi.org/10.1016/S0010-8545(00)00309-X.

7 Vogler, A.; Kunkely, H. Photoreactivity of Metal-to-Ligand Charge Transfer Excited States. *Coord. Chem. Rev.* **1998**, *177* (1), 81–96. https://doi.org/10.1016/S0010-8545(98)00131-3.

8 Vlček, A. Mechanistic Roles of Metal-to-Ligand Charge-Transfer Excited States in Organometallic Photochemistry. *Coord. Chem. Rev.* **1998**, *177* (1), 219–256. https://doi.org/10.1016/S0010-8545(98)00187-8.

9 Vogler, A.; Kunkely, H. Excited State Properties of Transition Metal Phosphine Complexes. *Coord. Chem. Rev.* **2002**, *230* (1), 243–251. https://doi.org/10.1016/S0010-8545(01)00438-6.

10 Wenger, O. S. Proton-Coupled Electron Transfer Originating from Excited States of Luminescent Transition-Metal Complexes. *Chem. – Eur. J.* **2011**, *17* (42), 11692–11702. https://doi.org/10.1002/chem.201102011.

11 Hicks, C.; Ye, G.; Levi, C.; Gonzales, M.; Rutenburg, I.; Fan, J.; Helmy, R.; Kassis, A.; Gafney, H. D. Excited-State Acid–Base Chemistry of Coordination Complexes. *Coord. Chem. Rev.* **2001**, *211* (1), 207–222. https://doi.org/10.1016/S0010-8545(00)00279-4.

12 Wenger, O. S. A Bright Future for Photosensitizers. *Nat. Chem.* **2020**, *12* (4), 323–324. https://doi.org/10.1038/s41557-020-0448-x.

13 Sinha, N.; Wenger, O. S. Photoactive Metal-to-Ligand Charge Transfer Excited States in 3d6 Complexes with Cr0, MnI, FeII, and CoIII. *J. Am. Chem. Soc.* **2023**, *145* (9), 4903–4920. https://doi.org/10.1021/jacs.2c13432.

14 Wegeberg, C.; Wenger, O. S. Luminescent First-Row Transition Metal Complexes. *JACS Au* **2021**, *1* (11), 1860–1876. https://doi.org/10.1021/jacsau.1c00353.

15 McCusker, J. K. Electronic Structure in the Transition Metal Block and Its Implications for Light Harvesting. *Science* **2019**, *363* (6426), 484–488. https://doi.org/10.1126/science.aav9104.

16 Wenger, O. S. Is Iron the New Ruthenium? *Chem. – Eur. J.* **2019**, *25* (24), 6043–6052. https://doi.org/10.1002/chem.201806148.

17 Thompson, D. W.; Ito, A.; Meyer, T. J. [Ru(bpy)3]2+* and other remarkable metal-to-ligand charge transfer (MLCT) excited states. *Pure Appl. Chem.* **2013**, *85* (7), 1257–1305. https://doi.org/10.1351/PAC-CON-13-03-04.

18 Trogler, W. C.; Erwin, D. K.; Geoffroy, G. L.; Gray, H. B. Production of Hydrogen by Ultraviolet Irradiation of Binuclear Molybdenum(II) Complexes in Acidic Aqueous Solutions. Observation of Molybdenum Hydride Intermediates in Octahalodimolybdate(II) Photoreactions. *J. Am. Chem. Soc.*

1978, *100* (4), 1160–1163. https://doi.org/10.1021/ja00472a020.
19 Hwang, S. J.; Powers, D. C.; Maher, A. G.; Anderson, B. L.; Hadt, R. G.; Zheng, S.-L.; Chen, Y.-S.; Nocera, D. G. Trap-Free Halogen Photoelimination from Mononuclear Ni(III) Complexes. *J. Am. Chem. Soc.* **2015**, *137* (20), 6472–6475. https://doi.org/10.1021/jacs.5b03192.
20 Lee, Y. F.; Kirchhoff, J. R. Absorption and Luminescence Spectroelectrochemical Characterization of a Highly Luminescent Rhenium(II) Complex. *J. Am. Chem. Soc.* **1994**, *116* (8), 3599–3600. https://doi.org/10.1021/ja00087a056.
21 Allmand, A. J.; Webb, W. W. CXCVII.—The Photolysis of Potassium Ferrioxalate Solutions. Part I. Experimental. *J. Chem. Soc. Resumed* **1929**, No. 0, 1518–1531. https://doi.org/10.1039/JR9290001518.
22 Zhang, Y.; Petersen, J. L.; Milsmann, C. A Luminescent Zirconium(IV) Complex as a Molecular Photosensitizer for Visible Light Photoredox Catalysis. *J. Am. Chem. Soc.* **2016**, *138* (40), 13115–13118. https://doi.org/10.1021/jacs.6b05934.
23 Erker, G. The Reaction of Intermediate Zirconocene-Aryne Complexes with C⍰H Bonds in the Thermolysis of Diarylzirconocenes. *J. Organomet. Chem.* **1977**, *134* (2), 189–202. https://doi.org/10.1016/S0022-328X(00)81419-9.
24 Carter, R. *Molecular Symmetry and Group Theory*; John Wiley & Sons, Ltd: Danvers, MA, 1998.
25 Haggag, O. S.; Malakar, P.; Pokhilko, P.; Stanton, J. F.; Krylov, A. I.; Ruhman, S. The Elusive Dynamics of Aqueous Permanganate Photochemistry. *Phys. Chem. Chem. Phys.* **2020**, *22* (18), 10043–10055. https://doi.org/10.1039/C9CP07028A.
26 Viste, A.; Gray, H. B. The Electronic Structure of Permanganate Ion. *Inorg. Chem.* **1964**, *3* (8), 1113–1123. https://doi.org/10.1021/ic50018a011.
27 Holt, S. L.; Ballhausen, C. J. Low Temperature Absorption Spectra of KMnO4 in KClo4. *Theor. Chim. Acta* **1967**, *7* (4), 313–320. https://doi.org/10.1007/BF00537508.
28 Glebov, E. M.; Pozdnyakov, I. P.; Plyusnin, V. F.; Khmelinskii, I. Primary Reactions in the Photochemistry of Hexahalide Complexes of Platinum Group Metals: A Minireview. *J. Photochem. Photobiol. C Photochem. Rev.* **2015**, *24*, 1–15. https://doi.org/10.1016/j.jphotochemrev.2015.05.003.
29 Jørgensen, Chr. K. Electron Transfer Spectra of Hexahalide Complexes. *Mol. Phys.* **1959**, *2* (3), 309–332. https://doi.org/10.1080/00268975900100291.
30 Budkina, D. S.; Gemeda, F. T.; Matveev, S. M.; Tarnovsky, A. N. Ultrafast Dynamics in LMCT and Intraconfigurational Excited States in Hexahaloiridates(IV), Models for Heavy Transition Metal Complexes and Building Blocks of Quantum Correlated Materials. *Phys. Chem. Chem. Phys.* **2020**, *22* (30), 17351–17364. https://doi.org/10.1039/D0CP00438C.
31 Kasha, M. Characterization of Electronic Transitions in Complex Molecules. *Discuss. Faraday Soc.* **1950**, *9* (0), 14–19. https://doi.org/10.1039/DF9500900014.
32 Braslavsky, S. E. Glossary of Terms Used in Photochemistry, 3rd Edition (IUPAC Recommendations 2006). *Pure Appl. Chem.* **2007**, *79* (3), 293–465. https://doi.org/10.1351/pac200779030293.
33 Lever, A. B. P. Charge Transfer Spectra of Transition Metal Complexes. *J. Chem. Educ.* **1974**, *51* (9), 612. https://doi.org/10.1021/ed051p612.
34 Matveev, S. M.; Budkina, D. S.; Zheldakov, I. L.; Phelan, M. R.; Hicks, C. M.; Tarnovsky, A. N. Femtosecond Dynamics of Metal-Centered and Ligand-to-Metal Charge-Transfer (T2g-Based) Electronic Excited States in Various Solvents: A Comprehensive Study of IrBr62−. *J. Chem. Phys.* **2019**, *150* (5), 054302. https://doi.org/10.1063/1.5079754.
35 Kunkely, H.; Vogler, A. Photoredox Reactivity of Iron(III) Phenolates in Aqueous Solution Induced by Ligand-to-Metal Charge Transfer Excitation. *Inorg. Chem. Commun.* **2003**, *6* (10), 1335–1337. https://doi.org/10.1016/j.inoche.2003.07.004.
36 Choi, E. H.; Ahn, D.-S.; Park, S.; Kim, C.; Ahn, C. W.; Kim, S.; Choi, M.; Yang, C.; Kim, T. W.; Ki, H.; Choi, J.; Pedersen, M. N.; Wulff, M.; Kim, J.; Ihee, H. Structural Dynamics of Bismuth Triiodide in Solution Triggered by Photoinduced Ligand-to-Metal Charge Transfer. *J. Phys. Chem. Lett.* **2019**, *10* (6), 1279–1285. https://doi.org/10.1021/acs.jpclett.9b00365.
37 Tonks, I. A.; Durrell, A. C.; Gray, H. B.; Bercaw, J. E. Groups 5 and 6 Terminal Hydrazido(2−) Complexes: Nβ Substituent Effects on Ligand-to-Metal Charge-Transfer Energies and Oxidation States. *J. Am. Chem. Soc.* **2012**, *134* (17), 7301–7304. https://doi.org/10.1021/ja302275j.
38 Kunkely, H.; Vogler, A. Photolysis of CH3Re(O2)2O Induced by Ligand-to-Metal Charge Transfer and by Peroxide Intraligand Excitation. *Inorg. Chem. Commun.* **2005**, *8* (5), 467–470. https://doi.org/10.1016/j.inoche.2005.02.014.
39 Lim, K. S.; Lee, D. Y.; Valencia, G. M.; Bull, D. A.; Won, Y.-W. Direct Incorporation of Functional Peptides into M-DNA through Ligand-to-Metal Charge Transfer. *ACS Macro Lett.* **2017**, *6* (2), 98–102. https://doi.org/10.1021/acsmacrolett.6b00865.
40 Kunkely, H.; Vogler, A. Photochemistry of Tris(Diethyldithiocarbamato)Iron(III). Reduction to a Stable Iron(II) Complex Induced by Ligand-to-Metal Charge Transfer Excitation. *Inorg. Chem. Commun.* **2002**, *5* (9), 730–732. https://doi.org/10.1016/S1387-7003(02)00555-5.
41 Kirchhoff, J. R.; Allen, M. R.; Cheesman, B. V.; Ken-ichi Okamoto; Heineman, W. R.; Deutsch, E. Electrochemistry and Spectroelectrochemistry of [Re(1,2-Bis(Dimethylphosphino)Ethane)3]+. *Inorganica Chim. Acta* **1997**, *262* (2), 195–202. https://doi.org/10.1016/S0020-1693(97)05523-0.
42 Del Negro, A. S.; Seliskar, C. J.; Heineman, W. R.; Hightower, S. E.; Bryan, S. A.; Sullivan, B. P. Highly Oxidizing Excited States of Re and Tc Complexes. *J. Am. Chem. Soc.* **2006**, *128* (51), 16494–16495. https://doi.org/10.1021/ja067114g.
43 Messersmith, S. J.; Kirschbaum, K.; Kirchhoff, J. R. Luminescent Low-Valent Rhenium Complexes with 1,2-Bis(Dialkylphosphino)Ethane Ligands. Synthesis and X-Ray Crystallographic, Electrochemical, and Spectroscopic Characterization. *Inorg. Chem.* **2010**, *49* (8), 3857–3865. https://doi.org/10.1021/ic902549b.
44 Chatterjee, S.; Del Negro, A. S.; Smith, F. N.; Wang, Z.; Hightower, S. E.; Sullivan, B. P.; Heineman, W. R.; Seliskar, C. J.; Bryan, S. A. Photophysics and Luminescence Spectroelectrochemistry of [Tc(Dmpe)3]+/2+ (Dmpe = 1,2-Bis(Dimethylphosphino)Ethane). *J. Phys. Chem. A* **2013**, *117* (48), 12749–12758. https://doi.org/10.1021/jp406365c.
45 Adams, J. J.; Arulsamy, N.; Sullivan, B. P.; Roddick, D. M.; Neuberger, A.; Schmehl, R. H. Homoleptic Tris-Diphosphine Re(I) and Re(II) Complexes and Re(II) Photophysics and Photochemistry. *Inorg. Chem.* **2015**, *54* (23), 11136–11149. https://doi.org/10.1021/acs.inorgchem.5b01395.
46 Zhang, Y.; Akhmedov, N. G.; Petersen, J. L.; Milsmann, C. Photoluminescence of Seven-Coordinate Zirconium and Hafnium Complexes with 2,2′-Pyridylpyrrolide Ligands. *Chem. – Eur. J.* **2019**, *25* (12), 3042–3052. https://doi.org/10.1002/chem.201804671.
47 Zhang, Y.; Lee, T. S.; Petersen, J. L.; Milsmann, C. A Zirconium Photosensitizer with a Long-Lived Excited State: Mechanistic Insight into Photoinduced Single-Electron Transfer. *J. Am. Chem. Soc.* **2018**, *140* (18), 5934–5947. https://doi.org/10.1021/jacs.8b00742.
48 Romain, C.; Choua, S.; Collin, J.-P.; Heinrich, M.; Bailly, C.; Karmazin-Brelot, L.; Bellemin-Laponnaz, S.; Dagorne, S. Redox and Luminescent Properties of Robust and Air-Stable N-

Heterocyclic Carbene Group 4 Metal Complexes. *Inorg. Chem.* **2014**, *53* (14), 7371–7376. https://doi.org/10.1021/ic500718y.

49 Kjær, K. S.; Kaul, N.; Prakash, O.; Chábera, P.; Rosemann, N. W.; Honarfar, A.; Gordivska, O.; Fredin, L. A.; Bergquist, K.-E.; Häggström, L.; Ericsson, T.; Lindh, L.; Yartsev, A.; Styring, S.; Huang, P.; Uhlig, J.; Bendix, J.; Strand, D.; Sundström, V.; Persson, P.; Lomoth, R.; Wärnmark, K. Luminescence and Reactivity of a Charge-Transfer Excited Iron Complex with Nanosecond Lifetime. *Science* **2019**, *363* (6424), 249–253. https://doi.org/10.1126/science.aau7160.

50 Chábera, P.; Liu, Y.; Prakash, O.; Thyrhaug, E.; Nahhas, A. E.; Honarfar, A.; Essén, S.; Fredin, L. A.; Harlang, T. C. B.; Kjær, K. S.; Handrup, K.; Ericson, F.; Tatsuno, H.; Morgan, K.; Schnadt, J.; Häggström, L.; Ericsson, T.; Sobkowiak, A.; Lidin, S.; Huang, P.; Styring, S.; Uhlig, J.; Bendix, J.; Lomoth, R.; Sundström, V.; Persson, P.; Wärnmark, K. A Low-Spin Fe(III) Complex with 100-Ps Ligand-to-Metal Charge Transfer Photoluminescence. *Nature* **2017**, *543* (7647), 695–699. https://doi.org/10.1038/nature21430.

51 Kaufhold, S.; Wärnmark, K. Design and Synthesis of Photoactive Iron N-Heterocyclic Carbene Complexes. *Catalysts* **2020**, *10* (1), 132. https://doi.org/10.3390/catal10010132.

52 Lindh, L.; Chábera, P.; Rosemann, N. W.; Uhlig, J.; Wärnmark, K.; Yartsev, A.; Sundström, V.; Persson, P. Photophysics and Photochemistry of Iron Carbene Complexes for Solar Energy Conversion and Photocatalysis. *Catalysts* **2020**, *10* (3), 315. https://doi.org/10.3390/catal10030315.

53 Harris, J. P.; Reber, C.; Colmer, H. E.; Jackson, T. A.; Forshaw, A. P.; Smith, J. M.; Kinney, R. A.; Telser, J. Near-Infrared 2Eg → 4A2g and Visible LMCT Luminescence from a Molecular Bis-(Tris(Carbene)Borate) Manganese(IV) Complex. *Can. J. Chem.* **2017**, *95* (5), 547–552. https://doi.org/10.1139/cjc-2016-0607.

54 Ericson, F.; Honarfar, A.; Prakash, O.; Tatsuno, H.; Fredin, L. A.; Handrup, K.; Chabera, P.; Gordivska, O.; Kjær, K. S.; Liu, Y.; Schnadt, J.; Wärnmark, K.; Sundström, V.; Persson, P.; Uhlig, J. Electronic Structure and Excited State Properties of Iron Carbene Photosensitizers – A Combined X-Ray Absorption and Quantum Chemical Investigation. *Chem. Phys. Lett.* **2017**, *683*, 559–566. https://doi.org/10.1016/j.cplett.2017.03.085.

55 Rodriguez, T. M.; Deegbey, M.; Chen, C.-H.; Jakubikova, E.; Dempsey, J. L. Isocyanide Ligands Promote Ligand-to-Metal Charge Transfer Excited States in a Rhenium(II) Complex. *Inorg. Chem.* **2023**. https://doi.org/10.1021/acs.inorgchem.2c03193.

56 Vogler, A.; Kunkely, H. Luminescence from Hexacyanoruthenate(III). *Inorganica Chim. Acta* **1981**, *53*, L215–L216. https://doi.org/10.1016/S0020-1693(00)84799-4.

57 Alexander, J. J.; Gray, H. B. Electronic Structures of Hexacyanometalate Complexes. *J. Am. Chem. Soc.* **1968**, *90* (16), 4260–4271. https://doi.org/10.1021/ja01018a013.

58 (58) Hahn, A. W.; Van Kuiken, B. E.; Chilkuri, V. G.; Levin, N.; Bill, E.; Weyhermüller, T.; Nicolaou, A.; Miyawaki, J.; Harada, Y.; DeBeer, S. Probing the Valence Electronic Structure of Low-Spin Ferrous and Ferric Complexes Using 2p3d Resonant Inelastic X-Ray Scattering (RIXS). *Inorg. Chem.* **2018**, *57* (15), 9515–9530. https://doi.org/10.1021/acs.inorgchem.8b01550.

59 Zhang, W.; Ji, M.; Sun, Z.; Gaffney, K. J. Dynamics of Solvent-Mediated Electron Localization in Electronically Excited Hexacyanoferrate(III). *J. Am. Chem. Soc.* **2012**, *134* (5), 2581–2588. https://doi.org/10.1021/ja207306t.

60 Avila, Y.; Acevedo-Peña, P.; Reguera, L.; Reguera, E. Recent Progress in Transition Metal Hexacyanometallates: From Structure to Properties and Functionality. *Coord. Chem. Rev.* **2022**, *453*, 214274. https://doi.org/10.1016/j.ccr.2021.214274.

61 Mann, K. R.; Cimolino, M.; Geoffroy, G. L.; Hammond, G. S.; Orio, A. A.; Albertin, G.; Gray, H. B. Electronic Structures and Spectra of Hexakisphenylisocyanide Complexes of Cr(0), Mo(0), W(0), Mn(I), and Mn(II). *Inorganica Chim. Acta* **1976**, *16*, 97–101. https://doi.org/10.1016/S0020-1693(00)91697-9.

62 Yarranton, J. T.; McCusker, J. K. Ligand-Field Spectroscopy of Co(III) Complexes and the Development of a Spectrochemical Series for Low-Spin D6 Charge-Transfer Chromophores. *J. Am. Chem. Soc.* **2022**, *144* (27), 12488–12500. https://doi.org/10.1021/jacs.2c04945.

63 Rodriguez, T. M.; Deegbey, M.; Jakubikova, E.; Dempsey, J. L. The Ligand-to-Metal Charge Transfer Excited State of [Re(Dmpe)3]2+. *Photosynth. Res.* **2022**, *151* (2), 155–161. https://doi.org/10.1007/s11120-021-00859-7.

64 May, A. M.; Deegbey, M.; Edme, K.; Lee, K. J.; Perutz, R. N.; Jakubikova, E.; Dempsey, J. L. Electronic Structure and Photophysics of Low Spin D5 Metallocenes. *Inorg. Chem.* **2024**, *63* (4), 1858–1866. https://doi.org/10.1021/acs.inorgchem.3c03451.

65 East, N. R.; Naumann, R.; Förster, C.; Ramanan, C.; Diezemann, G.; Heinze, K. Oxidative Two-State Photoreactivity of a Manganese(IV) Complex Using near-Infrared Light. *Nat. Chem.* **2024**, 1–8. https://doi.org/10.1038/s41557-024-01446-8.

66 Loukova, G. V.; Huhn, W.; Vasiliev, V. P.; Smirnov, V. A. Ligand-to-Metal Charge Transfer Excited States with Unprecedented Luminescence Yield in Fluid Solution. *J. Phys. Chem. A* **2007**, *111* (20), 4117–4121. https://doi.org/10.1021/jp0721797.

67 Alt, H.; Rausch, M. D. Photochemical Reactions of Dimethyl Derivatives of Titanocene, Zirconocene, and Hafnocene. *J. Am. Chem. Soc.* **1974**, *96* (18), 5936–5937. https://doi.org/10.1021/ja00825a041.

68 Margulieux, G. W.; Semproni, S. P.; Chirik, P. J. Photochemically Induced Reductive Elimination as a Route to a Zirconocene Complex with a Strongly Activated N2 Ligand. *Angew. Chem. Int. Ed.* **2014**, *53* (35), 9189–9192. https://doi.org/10.1002/anie.201402401.

69 Tsai, Z.-T.; Brubaker, C. H. Photolysis of Titanocene Dichloride. *J. Organomet. Chem.* **1979**, *166* (2), 199–210. https://doi.org/10.1016/S0022-328X(00)91634-6.

70 Kenney, J. W. I.; Boone, D. R.; Striplin, D. R.; Chen, Y. H.; Hamar, K. B. Electronic Luminescence Spectra of Charge Transfer States of Titanium(IV) Metallocenes. *Organometallics* **1993**, *12* (9), 3671–3676. https://doi.org/10.1021/om00033a045.

71 Harrigan, R. W.; Hammond, G. S.; Gray, H. B. Photochemistry of Titanocene(IV) Derivatives. *J. Organomet. Chem.* **1974**, *81* (1), 79–85. https://doi.org/10.1016/S0022-328X(00)87889-4.

72 Tumas, W.; Wheeler, D. R.; Grubbs, R. H. Photochemistry of Titanacyclobutanes. Evidence for a Metal-Centered 1,4-Biradical Intermediate. *J. Am. Chem. Soc.* **1987**, *109* (20), 6182–6184. https://doi.org/10.1021/ja00254a048.

73 Patrick, E. L.; Ray, C. J.; Meyer, G. D.; Ortiz, T. P.; Marshall, J. A.; Brozik, J. A.; Summers, M. A.; Kenney, J. W. Non-Localized Ligand-to-Metal Charge Transfer Excited States in (Cp)2Ti(IV)(NCS)2. *J. Am. Chem. Soc.* **2003**, *125* (18), 5461–5470. https://doi.org/10.1021/ja028769u.

74 Pfennig, B. W.; Thompson, M. E.; Bocarsly, A. B. A New Class of Room Temperature Luminescent Organometallic Complexes: Luminescence and Photophysical Properties of Permethylscandocene Chloride in Fluid Solution. *J. Am. Chem. Soc.* **1989**, *111* (24), 8947–8948. https://doi.org/10.1021/ja00206a044.

75 Pfennig, B. W.; Thompson, M. E.; Bocarsly, A. B. Luminescent D0 Scandocene Complexes: Photophysical Studies and

Electronic Structure Calculations on Cp*2ScX (X = Cl, I, Me). *Organometallics* **1993**, *12* (3), 649–655. https://doi.org/10.1021/om00027a014.

76 Paulson, S.; Sullivan, B. P.; Caspar, J. V. Luminescent Ligand-to-Metal Charge-Transfer Excited States Based on Pentamethylcyclopentadienyl Complexes of Tantalum. *J. Am. Chem. Soc.* **1992**, *114* (17), 6905–6906. https://doi.org/10.1021/ja00043a040.

77 Zhang, Y.; Lee, T. S.; Favale, J. M.; Leary, D. C.; Petersen, J. L.; Scholes, G. D.; Castellano, F. N.; Milsmann, C. Delayed Fluorescence from a Zirconium(IV) Photosensitizer with Ligand-to-Metal Charge-Transfer Excited States. *Nat. Chem.* **2020**, *12* (4), 345–352. https://doi.org/10.1038/s41557-020-0430-7.

78 Heinselman, K. S.; Hopkins, M. D. Luminescence Properties of D0 Metal-Imido Compounds. *J. Am. Chem. Soc.* **1995**, *117* (49), 12340–12341. https://doi.org/10.1021/ja00154a039.

79 Dorn, M.; Kalmbach, J.; Boden, P.; Päpcke, A.; Gómez, S.; Förster, C.; Kuczelinis, F.; Carrella, L. M.; Büldt, L. A.; Bings, N. H.; Rentschler, E.; Lochbrunner, S.; González, L.; Gerhards, M.; Seitz, M.; Heinze, K. A Vanadium(III) Complex with Blue and NIR-II Spin-Flip Luminescence in Solution. *J. Am. Chem. Soc.* **2020**, *142* (17), 7947–7955. https://doi.org/10.1021/jacs.0c02122.

80 Reichenauer, F.; Wang, C.; Förster, C.; Boden, P.; Ugur, N.; Báez-Cruz, R.; Kalmbach, J.; Carrella, L. M.; Rentschler, E.; Ramanan, C.; Niedner-Schatteburg, G.; Gerhards, M.; Seitz, M.; Resch-Genger, U.; Heinze, K. Strongly Red-Emissive Molecular Ruby [Cr(Bpmp)2]3+ Surpasses [Ru(Bpy)3]2+. *J. Am. Chem. Soc.* **2021**, *143* (30), 11843–11855. https://doi.org/10.1021/jacs.1c05971.

81 Jiménez, J.-R.; Doistau, B.; Cruz, C. M.; Besnard, C.; Cuerva, J. M.; Campaña, A. G.; Piguet, C. Chiral Molecular Ruby [Cr(Dqp)2]3+ with Long-Lived Circularly Polarized Luminescence. *J. Am. Chem. Soc.* **2019**, *141* (33), 13244–13252. https://doi.org/10.1021/jacs.9b06524.

82 Kitzmann, W. R.; Moll, J.; Heinze, K. Spin-Flip Luminescence. *Photochem. Photobiol. Sci.* **2022**, *21* (7), 1309–1331. https://doi.org/10.1007/s43630-022-00186-3.

83 Bursten, B. E.; Cotton, F. A.; Fanwick, P. E.; Stanley, G. G. A Molecular Orbital Calculation of the Octachlorodirhenate(2-) Ion by the Relativistic SCF-X.Alpha.-SW Method. Redetermination and Reassignment of the Electronic Absorption Spectrum. *J. Am. Chem. Soc.* **1983**, *105* (10), 3082–3087. https://doi.org/10.1021/ja00348a022.

84 Kitzmann, W. R.; Heinze, K. Charge-Transfer and Spin-Flip States: Thriving as Complements. *Angew. Chem. Int. Ed.* **2023**, *62* (15), e202213207. https://doi.org/10.1002/anie.202213207.

85 Shiang, J. J.; Cole, A. G.; Sension, R. J.; Hang, K.; Weng, Y.; Trommel, J. S.; Marzilli, L. G.; Lian, T. Ultrafast Excited-State Dynamics in Vitamin B12 and Related Cob(III)Alamins. *J. Am. Chem. Soc.* **2006**, *128* (3), 801–808. https://doi.org/10.1021/ja054374+.

86 Pal, A. K.; Li, C.; Hanan, G. S.; Zysman-Colman, E. Blue-Emissive Cobalt(III) Complexes and Their Use in the Photocatalytic Trifluoromethylation of Polycyclic Aromatic Hydrocarbons. *Angew. Chem. Int. Ed.* **2018**, *57* (27), 8027–8031. https://doi.org/10.1002/anie.201802532.

87 Schrauzer, G. N.; Lee, L.-P.; Sibert, J. W. Alkylcobalamins and Alkylcobaloximes. Electronic Structure, Spectra, and Mechanism of Photodealkylation. *J. Am. Chem. Soc.* **1970**, *92* (10), 2997–3005. https://doi.org/10.1021/ja00713a012.

88 Engl, S.; Reiser, O. Making Copper Photocatalysis Even More Robust and Economic: Photoredox Catalysis with [CuII(Dmp)2Cl]Cl. *Eur. J. Org. Chem.* **2020**, *2020* (10), 1523–1533. https://doi.org/10.1002/ejoc.201900839.

89 Reichle, A.; Reiser, O. Light-Induced Homolysis of Copper(Ii)-Complexes – a Perspective for Photocatalysis. *Chem. Sci.* **2023**, *14* (17), 4449–4462. https://doi.org/10.1039/D3SC00388D.

90 Ravetz, B. D.; Wang, J. Y.; Ruhl, K. E.; Rovis, T. Photoinduced Ligand-to-Metal Charge Transfer Enables Photocatalyst-Independent Light-Gated Activation of Co(II). *ACS Catal.* **2019**, *9* (1), 200–204. https://doi.org/10.1021/acscatal.8b04326.

91 Xu, P.; López-Rojas, P.; Ritter, T. Radical Decarboxylative Carbometalation of Benzoic Acids: A Solution to Aromatic Decarboxylative Fluorination. *J. Am. Chem. Soc.* **2021**, *143* (14), 5349–5354. https://doi.org/10.1021/jacs.1c02490.

92 Abderrazak, Y.; Bhattacharyya, A.; Reiser, O. Visible-Light-Induced Homolysis of Earth-Abundant Metal-Substrate Complexes: A Complementary Activation Strategy in Photoredox Catalysis. *Angew. Chem. Int. Ed.* **2021**, *60* (39), 21100–21115. https://doi.org/10.1002/anie.202100270.

93 Hossain, A.; Vidyasagar, A.; Eichinger, C.; Lankes, C.; Phan, J.; Rehbein, J.; Reiser, O. Visible-Light-Accelerated Copper(II)-Catalyzed Regio- and Chemoselective Oxo-Azidation of Vinyl Arenes. *Angew. Chem. Int. Ed.* **2018**, *57* (27), 8288–8292. https://doi.org/10.1002/anie.201801678.

94 Hwang, S. J.; Anderson, B. L.; Powers, D. C.; Maher, A. G.; Hadt, R. G.; Nocera, D. G. Halogen Photoelimination from Monomeric Nickel(III) Complexes Enabled by the Secondary Coordination Sphere. *Organometallics* **2015**, *34* (19), 4766–4774. https://doi.org/10.1021/acs.organomet.5b00568.

95 Gonzalez, M. I.; Gygi, D.; Qin, Y.; Zhu, Q.; Johnson, E. J.; Chen, Y.-S.; Nocera, D. G. Taming the Chlorine Radical: Enforcing Steric Control over Chlorine-Radical-Mediated C–H Activation. *J. Am. Chem. Soc.* **2022**, *144* (3), 1464–1472. https://doi.org/10.1021/jacs.1c13333.

96 Balakrishnan, G.; Soldatova, A. V.; Reid, P. J.; Spiro, T. G. Ultrafast Charge Transfer in Nickel Phthalocyanine Probed by Femtosecond Raman-Induced Kerr Effect Spectroscopy. *J. Am. Chem. Soc.* **2014**, *136* (24), 8746–8754. https://doi.org/10.1021/ja503541v.

97 Prather, K. V.; Tsui, E. Y. Photoinduced Ligand-to-Metal Charge Transfer of Cobaltocene: Radical Release and Catalytic Cyclotrimerization. *Inorg. Chem.* **2023**, *62* (5), 2128–2134. https://doi.org/10.1021/acs.inorgchem.2c03779.

98 Treacy, S. M.; Rovis, T. Copper Catalyzed C(Sp3)–H Bond Alkylation via Photoinduced Ligand-to-Metal Charge Transfer. *J. Am. Chem. Soc.* **2021**, *143* (7), 2729–2735. https://doi.org/10.1021/jacs.1c00687.

99 Costanzo, L. L.; Pistarà, S.; Condorelli, G. Photoreduction of Cerium(IV) Hexachloride in Acetonitrile. *J. Photochem.* **1983**, *21* (1), 45–51. https://doi.org/10.1016/0047-2670(83)80006-9.

100 Qiao, Y.; Yin, H.; M. Moreau, L.; Feng, R.; F. Higgins, R.; C. Manor, B.; J. Carroll, P.; H. Booth, C.; Autschbach, J.; J. Schelter, E. Cerium(Iv) Complexes with Guanidinate Ligands: Intense Colors and Anomalous Electronic Structures. *Chem. Sci.* **2021**, *12* (10), 3558–3567. https://doi.org/10.1039/D0SC05193D.

101 Da Re, R. E.; Kuehl, C. J.; Brown, M. G.; Rocha, R. C.; Bauer, E. D.; John, K. D.; Morris, D. E.; Shreve, A. P.; Sarrao, J. L. Electrochemical and Spectroscopic Characterization of the Novel Charge-Transfer Ground State in Diimine Complexes of Ytterbocene. *Inorg. Chem.* **2003**, *42* (18), 5551–5559. https://doi.org/10.1021/ic030069i.

102 Petoud, S.; Bünzli, J.-C. G.; Glanzman, T.; Piguet, C.; Xiang, Q.; Thummel, R. P. Influence of Charge-Transfer States on the Eu(III) Luminescence in Mononuclear Triple Helical Complexes with Tridentate Aromatic Ligands. *J. Lumin.* **1999**, *82* (1), 69–79. https://doi.org/10.1016/S0022-2313(99)00015-0.

103 Mürner, H.-R.; Chassat, E.; Thummel, R. P.; Bünzli, J.-C. G. Strong Enhancement of the Lanthanide-Centred

Luminescence in Complexes with 4-Alkylated 2,2′;6′,2′′-Terpyridines. *J. Chem. Soc. Dalton Trans.* **2000**, No. 16, 2809–2816. https://doi.org/10.1039/B003577G.

104 Shirase, S.; Tamaki, S.; Shinohara, K.; Hirosawa, K.; Tsurugi, H.; Satoh, T.; Mashima, K. Cerium(IV) Carboxylate Photocatalyst for Catalytic Radical Formation from Carboxylic Acids: Decarboxylative Oxygenation of Aliphatic Carboxylic Acids and Lactonization of Aromatic Carboxylic Acids. *J. Am. Chem. Soc.* **2020**, *142* (12), 5668–5675. https://doi.org/10.1021/jacs.9b12918.

105 Rousset, E.; Piccardo, M.; Gable, R. W.; Massi, M.; Sorace, L.; Soncini, A.; Boskovic, C. Elucidation of LMCT Excited States for Lanthanoid Complexes: A Theoretical and Solid-State Experimental Framework. *Inorg. Chem.* **2022**, *61* (35), 14004–14018. https://doi.org/10.1021/acs.inorgchem.2c01985.

106 Qiao, Y.; Yang, Q.; Schelter, E. J. Photoinduced Miyaura Borylation by a Rare-Earth-Metal Photoreductant: The Hexachlorocerate(III) Anion. *Angew. Chem. Int. Ed.* **2018**, *57* (34), 10999–11003. https://doi.org/10.1002/anie.201804022.

107 Yang, Q.; Wang, Y.-H.; Qiao, Y.; Gau, M.; Carroll, P. J.; Walsh, P. J.; Schelter, E. J. Photocatalytic C–H Activation and the Subtle Role of Chlorine Radical Complexation in Reactivity. *Science* **2021**, *372* (6544), 847–852. https://doi.org/10.1126/science.abd8408.

108 Zhang, K.; Chang, L.; An, Q.; Wang, X.; Zuo, Z. Dehydroxymethylation of Alcohols Enabled by Cerium Photocatalysis. *J. Am. Chem. Soc.* **2019**, *141* (26), 10556–10564. https://doi.org/10.1021/jacs.9b05932.

109 Bian, K.-J.; Kao, S.-C.; Nemoto, D.; Chen, X.-W.; West, J. G. Photochemical Diazidation of Alkenes Enabled by Ligand-to-Metal Charge Transfer and Radical Ligand Transfer. *Nat. Commun.* **2022**, *13* (1), 7881. https://doi.org/10.1038/s41467-022-35560-3.

110 Zhang, M.; Zhang, J.; Li, Q.; Shi, Y. Iron-Mediated Ligand-to-Metal Charge Transfer Enables 1,2-Diazidation of Alkenes. *Nat. Commun.* **2022**, *13* (1), 7880. https://doi.org/10.1038/s41467-022-35344-9.

111 Lu, Y.-C.; West, J. G. Chemoselective Decarboxylative Protonation Enabled by Cooperative Earth-Abundant Element Catalysis. *Angew. Chem. Int. Ed.* **2023**, *62* (3), e202213055. https://doi.org/10.1002/anie.202213055.

112 Hatchard, C. G.; Parker, C. A.; Bowen, E. J. A New Sensitive Chemical Actinometer - II. Potassium Ferrioxalate as a Standard Chemical Actinometer. *Proc. R. Soc. Lond. Ser. Math. Phys. Sci.* **1997**, *235* (1203), 518–536. https://doi.org/10.1098/rspa.1956.0102.

113 Parker, C. A.; Bowen, E. J. A New Sensitive Chemical Actinometer. I. Some Trials with Potassium Ferrioxalate. *Proc. R. Soc. Lond. Ser. Math. Phys. Sci.* **1997**, *220* (1140), 104–116. https://doi.org/10.1098/rspa.1953.0175.

114 Bowman, W. D.; Demas, J. N. Ferrioxalate Actinometry. A Warning on Its Correct Use. *J. Phys. Chem.* **1976**, *80* (21), 2434–2435. https://doi.org/10.1021/j100562a025.

115 Pozdnyakov, I. P.; Kel, O. V.; Plyusnin, V. F.; Grivin, V. P.; Bazhin, N. M. New Insight into Photochemistry of Ferrioxalate. *J. Phys. Chem. A* **2008**, *112* (36), 8316–8322. https://doi.org/10.1021/jp8040583.

116 Ogi, Y.; Obara, Y.; Katayama, T.; Suzuki, Y.-I.; Liu, S. Y.; Bartlett, N. C.-M.; Kurahashi, N.; Karashima, S.; Togashi, T.; Inubushi, Y.; Ogawa, K.; Owada, S.; Rubešová, M.; Yabashi, M.; Misawa, K.; Slavíček, P.; Suzuki, T. Ultraviolet Photochemical Reaction of [Fe(III)(C2O4)3]3− in Aqueous Solutions Studied by Femtosecond Time-Resolved X-Ray Absorption Spectroscopy Using an X-Ray Free Electron Laser. *Struct. Dyn.* **2015**, *2* (3), 034901. https://doi.org/10.1063/1.4918803.

117 Li, X.; Hou, M.; Fu, Y.; Wang, L.; Wang, Y.; Lin, D.; Li, Q.; Hu, D.; Wang, Z. A Chronological Review of Photochemical Reactions of Ferrioxalate at the Molecular Level: New Insights into an Old Story. *Chin. Chem. Lett.* **2023**, *34* (5), 107752. https://doi.org/10.1016/j.cclet.2022.107752.

118 Parker, C. A. Induced Autoxidation of Oxalate in Relation to the Photolysis of Potassium Ferrioxalate. *Trans. Faraday Soc.* **1954**, *50* (0), 1213–1221. https://doi.org/10.1039/TF9545001213.

119 Chen, J.; Browne, W. R. Photochemistry of Iron Complexes. *Coord. Chem. Rev.* **2018**, *374*, 15–35. https://doi.org/10.1016/j.ccr.2018.06.008.

120 Mangiante, D. M.; Schaller, R. D.; Zarzycki, P.; Banfield, J. F.; Gilbert, B. *Mechanism of Ferric Oxalate Photolysis*. ACS Publications. https://doi.org/10.1021/acsearthspacechem.7b00026.

121 Weller, C.; Horn, S.; Herrmann, H. Photolysis of Fe(III) Carboxylato Complexes: Fe(II) Quantum Yields and Reaction Mechanisms. *J. Photochem. Photobiol. Chem.* **2013**, *268*, 24–36. https://doi.org/10.1016/j.jphotochem.2013.06.022.

122 Bock, C. R.; Connor, J. A.; Gutierrez, A. R.; Meyer, T. J.; Whitten, D. G.; Sullivan, B. P.; Nagle, J. K. Estimation of Excited-State Redox Potentials by Electron-Transfer Quenching. Application of Electron-Transfer Theory to Excited-State Redox Processes. *J. Am. Chem. Soc.* **1979**, *101* (17), 4815–4824. https://doi.org/10.1021/ja00511a007.

123 Aydogan, A.; Bangle, R. E.; Cadranel, A.; Turlington, M. D.; Conroy, D. T.; Cauët, E.; Singleton, M. L.; Meyer, G. J.; Sampaio, R. N.; Elias, B.; Troian-Gautier, L. Accessing Photoredox Transformations with an Iron(III) Photosensitizer and Green Light. *J. Am. Chem. Soc.* **2021**, *143* (38), 15661–15673. https://doi.org/10.1021/jacs.1c06081.

124 Deng, Y.; Seliskar, C. J.; Heineman, W. R. Electrochemical Behavior of [ReI(DMPE)3]+, Where DMPE = 1,2-Bis(Dimethylphosphino)Ethane, at Perfluorosulfonated Ionomer-Modified Electrodes. *Anal. Chem.* **1997**, *69* (19), 4045–4050. https://doi.org/10.1021/ac961295v.

125 Zhang, Y.; Leary, D. C.; Belldina, A. M.; Petersen, J. L.; Milsmann, C. Effects of Ligand Substitution on the Optical and Electrochemical Properties of (Pyridinedipyrrolide)Zirconium Photosensitizers. *Inorg. Chem.* **2020**, *59* (20), 14716–14730. https://doi.org/10.1021/acs.inorgchem.0c02343.

126 Durham, B.; Caspar, J. V.; Nagle, J. K.; Meyer, T. J. Photochemistry of Tris(2,2′-Bipyridine)Ruthenium(2+) Ion. *J. Am. Chem. Soc.* **1982**, *104* (18), 4803–4810. https://doi.org/10.1021/ja00382a012.

127 Bandy, J. A.; Cloke, F. G. N.; Copper, Glyn.; Day, J. P.; Girling, R. B.; Graham, R. G.; Green, J. C.; Grinter, Roger.; Perutz, R. N. Decamethylrhenocene, (.Eta.5-C5Me5)2Re. *J. Am. Chem. Soc.* **1988**, *110* (15), 5039–5050. https://doi.org/10.1021/ja00223a023.

128 Gazi, S.; Ng, W. K. H.; Ganguly, R.; Moeljadi, A. M. P.; Hirao, H.; Soo, H. S. Selective Photocatalytic C–C Bond Cleavage under Ambient Conditions with Earth Abundant Vanadium Complexes. *Chem. Sci.* **2015**, *6* (12), 7130–7142. https://doi.org/10.1039/C5SC02923F.

129 Barker, M.; Whittemore, T. J.; London, H. C.; Sledesky, J. M.; Harris, E. A.; Smith Pellizzeri, T. M.; McMillen, C. D.; Wagenknecht, P. S. Design Strategies for Luminescent Titanocenes: Improving the Photoluminescence and Photostability of Arylethynyltitanocenes. *Inorg. Chem.* **2023**, *62* (43), 17870–17882. https://doi.org/10.1021/acs.inorgchem.3c02712.

130 Prakash, O.; Lindh, L.; Kaul, N.; Rosemann, N. W.; Losada, I. B.; Johnson, C.; Chábera, P.; Ilic, A.; Schwarz, J.; Gupta, A. K.; Uhlig, J.; Ericsson, T.; Häggström, L.; Huang, P.; Bendix, J.; Strand, D.; Yartsev, A.; Lomoth, R.; Persson, P.; Wärnmark, K. Photophysical Integrity of the Iron(III) Scorpionate Framework in Iron(III)–NHC Complexes with Long-Lived 2LMCT Excited

States. *Inorg. Chem.* **2022**, *61* (44), 17515–17526. https://doi.org/10.1021/acs.inorgchem.2c02410.

131 Rosemann, N. W.; Chábera, P.; Prakash, O.; Kaufhold, S.; Wärnmark, K.; Yartsev, A.; Persson, P. Tracing the Full Bimolecular Photocycle of Iron(III)–Carbene Light Harvesters in Electron-Donating Solvents. *J. Am. Chem. Soc.* **2020**, *142* (19), 8565–8569. https://doi.org/10.1021/jacs.0c00755.

132 Bino, A.; Ardon, M. Unusual Reactions of a Bridged Hydride Ligand in Aqueous Solution. *J. Am. Chem. Soc.* **1977**, *99* (19), 6446–6447. https://doi.org/10.1021/ja00461a049.

133 Cotton, F. Albert.; Kalbacher, B. J. Oxidative Addition of Hydrohalic Acids to Dimolybdenum(II) Species. Reformulation of Mo2X83- as Mo2X8H3-. *Inorg. Chem.* **1976**, *15* (3), 522–524. https://doi.org/10.1021/ic50157a007.

134 Norman, J. G. Jr.; Kolari, H. J. Electronic Structure of Octachlorodimolybdate(II). *J. Am. Chem. Soc.* **1975**, *97* (1), 33–37. https://doi.org/10.1021/ja00834a008.

135 Simandiras, E. D.; Psaroudakis, N.; Mertis, K. Which Component of the Quadruple Bond Breaks First upon Protonation of the Octachlorodimetallate Anions [MM'Cl8]4−, M,M'=Mo, W? A Theoretical Study of Reactivity, Mechanism and Bonding. *Polyhedron* **2013**, *54*, 173–179. https://doi.org/10.1016/j.poly.2013.02.019.

136 Vilarrubias, P. Electronic Structure and Spectroscopy of Homoleptic Compounds of Dimolybdenum Using TDDFT. *Can. J. Chem.* **2016**, *94* (1), 20–27. https://doi.org/10.1139/cjc-2015-0210.

137 Gell, K. I.; Harris, T. V.; Schwartz, J. Synthesis and Characterization of Dimeric Zirconium(III) Complexes. Structure of "Zirconocene." *Inorg. Chem.* **1981**, *20* (2), 481–488. https://doi.org/10.1021/ic50216a033.

138 London, H. C.; Pritchett, D. Y.; Pienkos, J. A.; McMillen, C. D.; Whittemore, T. J.; Bready, C. J.; Myers, A. R.; Vieira, N. C.; Harold, S.; Shields, G. C.; Wagenknecht, P. S. Photochemistry and Photophysics of Charge-Transfer Excited States in Emissive D10/D0 Heterobimetallic Titanocene Tweezer Complexes. *Inorg. Chem.* **2022**, *61* (28), 10986–10998. https://doi.org/10.1021/acs.inorgchem.2c01746.

139 Roloff, A.; Meier, K.; Riediker, M. Synthetic and Metal Organic Photochemistry in Industry. *Pure Appl. Chem.* **1986**, *58* (9), 1267–1272. https://doi.org/10.1351/pac198658091267.

140 London, H. C.; Whittemore, T. J.; Gale, A. G.; McMillen, C. D.; Pritchett, D. Y.; Myers, A. R.; Thomas, H. D.; Shields, G. C.; Wagenknecht, P. S. Ligand-to-Metal Charge-Transfer Photophysics and Photochemistry of Emissive D0 Titanocenes: A Spectroscopic and Computational Investigation. *Inorg. Chem.* **2021**, *60* (18), 14399–14409. https://doi.org/10.1021/acs.inorgchem.1c02182.

141 Turlington, M. D.; Pienkos, J. A.; Carlton, E. S.; Wroblewski, K. N.; Myers, A. R.; Trindle, C. O.; Altun, Z.; Rack, J. J.; Wagenknecht, P. S. Complexes with Tunable Intramolecular Ferrocene to TiIV Electronic Transitions: Models for Solid State FeII to TiIV Charge Transfer. *Inorg. Chem.* **2016**, *55* (5), 2200–2211. https://doi.org/10.1021/acs.inorgchem.5b02587.

142 Pourreau, D. B.; Geoffroy, G. L. Photochemistry of Alkyl, Alkylidene, and Alkylidyne Complexes of the Transition Metals. In *Advances in Organometallic Chemistry*; Stone, F. G. A., West, R., Eds.; Academic Press, 1985; Vol. 24, pp 249–352. https://doi.org/10.1016/S0065-3055(08)60417-7.

143 Sikora, D. J.; Rausch, M. D. Reactions of Cp2M(CO)2 and Cp2M(CO)(PPh3) (M = Zr, Hf) with Acetylenes: Formation of Some Metallacyclopentadiene Complexes of Zirconocene and Hafnocene. *J. Organomet. Chem.* **1984**, *276* (1), 21–37. https://doi.org/10.1016/0022-328X(84)80601-4.

144 Brintzinger, H.; Bercaw, J. E. Nature of So-Called Titanocene, (C10H10Ti)2. *J. Am. Chem. Soc.* **1970**, *92* (21), 6182–6185. https://doi.org/10.1021/ja00724a013.

145 Pool, J. A.; Bernskoetter, W. H.; Chirik, P. J. On the Origin of Dinitrogen Hydrogenation Promoted by [(H5-C5Me4H)2Zr]2(M2,H2,H2-N2). *J. Am. Chem. Soc.* **2004**, *126* (44), 14326–14327. https://doi.org/10.1021/ja045566s.

146 Đỗ, P. M. N.; Akhmedov, N. G.; Petersen, J. L.; Dolinar, B. S.; Milsmann, C. Photochemical Synthesis of a Zirconium Cyclobutadienyl Complex. *Chem. Commun.* **2020**, *56* (40), 5397–5400. https://doi.org/10.1039/D0CC01104E.